Evidence for mechanical and chemical alteration of iron-nickel meteorites on Mars: Process insights for Meridiani Planum

J. W. Ashley,[1] M. P. Golombek,[2] P. R. Christensen,[1] S. W. Squyres,[3] T. J. McCoy,[4] C. Schröder,[5] I. Fleischer,[6] J. R. Johnson,[7] K. E. Herkenhoff,[7] and T. J. Parker[2]

Received 3 June 2010; revised 13 December 2010; accepted 28 December 2010; published 16 April 2011.

[1] The weathering of meteorites found on Mars involves chemical and physical processes that can provide clues to climate conditions at the location of their discovery. Beginning on sol 1961, the Opportunity rover encountered three large iron meteorites within a few hundred meters of each other. In order of discovery, these rocks have been assigned the unofficial names Block Island, Shelter Island, and Mackinac Island. Each rock presents a unique but complimentary set of features that increase our understanding of weathering processes at Meridiani Planum. Significant morphologic characteristics interpretable as weathering features include (1) a large pit in Block Island, lined with delicate iron protrusions suggestive of inclusion removal by corrosive interaction; (2) differentially eroded kamacite and taenite lamellae in Block Island and Shelter Island, providing relative timing through crosscutting relationships with deposition of (3) an iron oxide–rich dark coating; (4) regmaglypted surfaces testifying to regions of minimal surface modification, with other regions in the same meteorites exhibiting (5) large-scale, cavernous weathering (in Shelter Island and Mackinac Island). We conclude that the current size of the rocks is approximate to their original postfall contours. Their morphology thus likely results from a combination of atmospheric interaction and postfall weathering effects. Among our specific findings is evidence supporting (1) at least one possible episode of aqueous acidic exposure for Block Island; (2) ripple migration over portions of the meteorites; (3) a minimum of two separate episodes of wind abrasion; alternating with (4) at least one episode of coating-forming chemical alteration, most likely at subzero temperatures.

Citation: Ashley, J. W., M. P. Golombek, P. R. Christensen, S. W. Squyres, T. J. McCoy, C. Schröder, I. Fleischer, J. R. Johnson, K. E. Herkenhoff, and T. J. Parker (2011), Evidence for mechanical and chemical alteration of iron-nickel meteorites on Mars: Process insights for Meridiani Planum, *J. Geophys. Res.*, *116*, E00F20, doi:10.1029/2010JE003672.

1. Introduction

[2] Meteorites on the surface of Mars can provide natural experiments for monitoring weathering processes on the Red Planet. Such alteration is less relevant to the meteorites themselves than to the assessment of past and present climatic conditions from their degree and type of weathering. Because we are likely to have samples of similar rocks in Earth-based collections, meteorites on other worlds are the experimental equivalent of artificially inserting highly sensitive, unweathered rocks with known properties into a surface environment, and allowing them to alter over their exposure lifetimes. On Mars, such a period could conceivably span billions of years, but also includes the potential for recording very recent events. If exposure time scales can be estimated through indirect means (or direct means in the case of a sample return), meteorites on the surface of Mars may thus provide a sensitive tool for probing the subtle behavior of wind and water over a range of Martian epochs.

[3] Predicted concentration mechanisms for meteoritical material on Mars modeled by *Bland and Smith* [2000] (later corroborated by *Chappelow and Sharpton* [2006a]) yielded promising expectations for meteorite recognition and subsequent analysis on Mars when combined with the capabilities of the NASA Mars Exploration Rovers' (MER; Spirit and Opportunity) instrument payloads. Up to Opportunity sol 1961, the two rovers had traversed approximately 25 km of cumulative odometry (7.7 km for Spirit, and 17.2 km for Opportunity), and had discovered at least 10 confirmed and

[1]Mars Space Flight Facility, School of Earth and Space Exploration, Arizona State University, Tempe, Arizona, USA.
[2]Jet Propulsion Laboratory, California Institute of Technology, Pasadena, California, USA.
[3]Department of Astronomy, Cornell University, Ithaca, New York, USA.
[4]Department of Mineral Sciences, National Museum of Natural History, Smithsonian Institution, Washington, DC, USA.
[5]Center for Applied Geoscience, Eberhard Karls University, Tübingen, Germany.
[6]Institut für Anorganische und Analytische Chemie, Johannes Gutenberg-Universität, Mainz, Germany.
[7]Astrogeology Science Center, U.S. Geological Survey, Flagstaff, Arizona, USA.

0148-0227/11/2010JE003672

Table 1. Meteorite Candidates Identified on Mars

Meteorite	Rover	First Sol Encountered	Type[a]	Instrumentation Employed
Barberton	Opportunity	121	stony iron	PancamNavcam
Heat Shield Rock[b]	Opportunity	339	IAB complex iron	MTES/Pancam/APXS/MB/MI
Allan Hills	Spirit	858	iron	MTES/Pancam/Navcam
Zhong Shan	Spirit	858	iron	MTES/Pancam/Navcam
Santa Catarina	Opportunity	1034	stony iron	MTES/Pancam/APXS/MB/MI
Joacaba	Opportunity	1046	stony iron	MTES/Navcam
Mafra	Opportunity	1151	stony iron	MTES/Navcam
Paloma	Opportunity	1190	stony iron	MTES/Navcam
Santorini	Opportunity	1713	stony iron	Pancam/APXS/MB/MI
Kasos	Opportunity	1889	stony iron	Pancam/APXS/MB/MI
Block Island	Opportunity	1961	IAB complex iron	Pancam/APXS/MB/MI
Shelter Island	Opportunity	2022	IAB complex iron	Pancam/APXS/MB/MI
Mackinac Island	Opportunity	2034	iron	PancamNavcam
Oileán Ruaidh	Opportunity	2368	iron	PancamNavcam
Ireland	Opportunity	2374	iron	PancamNavcam

[a]Type is suspected or confirmed.
[b]Official name is Meridiani Planum [*Connolly et al.*, 2006].

candidate meteorites. In addition to the meteorite pair Allan Hills and Zhong Shan discovered by Spirit at Gusev crater [*Ruff et al.*, 2008], Meridiani meteorite candidates included Barberton [*Schröder et al.*, 2006]; Meridiani Planum (referred to hereafter by its original name of Heat Shield Rock to avoid confusion with the location name) and Santa Catarina [*Schröder et al.*, 2008]; Joacaba, Paloma, and Mafra [*Ashley et al.*, 2009b]; Santorini [*Schröder et al.*, 2009a]; and Kasos [*Schröder et al.*, 2010]. More recently (on sols 2368 and 2374), Opportunity encountered the Oileán Ruaidh and Ireland meteorites. See Table 1 for a list of these rocks and the instrumentation employed for each. With the exception of Heat Shield Rock (identified as a iron-nickel meteorite of the IAB complex [*Connolly et al.*, 2006]), the Meridiani finds up to sol 1961 were of a stony iron variety that may or may not be entirely meteoritic (their textures suggest the possibility of impact breccias that merely contain meteoritic minerals).

[4] Beginning on Opportunity sol 1961, three large iron-nickel meteorites were identified at locations less than 1 km from each other near the Nimrod ghost crater, located approximately 4.2 km SSW of Victoria crater (Figure 1). In

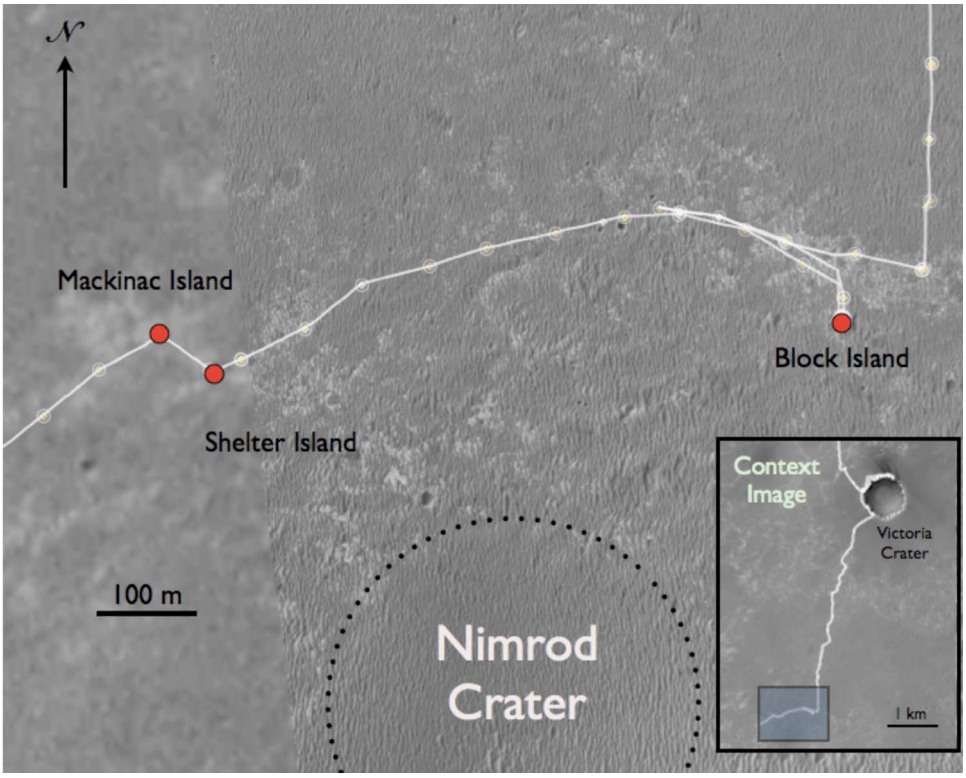

Figure 1. Site location map prepared from Mars Reconnaissance Orbiter/HiRISE image, showing positions of three iron-nickel meteorites and their relationship to the Nimrod ghost crater at Meridiani Planum. Inset shows context for the traverse from Victoria crater.

order of discovery, these have been assigned the unofficial names of Block Island, Shelter Island, and Mackinac Island (Table 1), and will be referred to collectively as the Meridiani iron suite, together with Heat Shield Rock. This paper focuses on data interpretations pursuant to the weathering history of these four meteorites (both Oileán Ruaidh and Ireland require further analysis). The Meridiani iron suite presents several lines of evidence to confirm both mechanical and chemical weathering processes at Meridiani Planum, and also helps resolve several outstanding questions raised by Heat Shield Rock. The phrase "Martian find" will be used in place of "Martian meteorite" to distinguish meteorites found on Mars from the SNC association of meteorites found on Earth, commonly also referred to as Martian meteorites. Related papers include discussions on meteorite mineralogy, composition, spectral properties, and delivery mechanisms [see *Fleischer et al.*, 2010b; *Schröder et al.*, 2010; *Weitz et al.*, 2010; *Chappelow and Golombek*, 2010b].

[5] The weathering of meteorites on another planet and its relevance to planetary science is an unusual set of topics that often raises a variety of multidisciplinary questions. Section 2.1 provides overview intended to address the more common of these. Readers may prefer to skip section 2.1 if already familiar with the material.

2. Background and General Overview of Meteorite Weathering Considerations

[6] The scientific value of meteorites is traditionally viewed in terms of their relevance to (1) the formation and evolutionary history of their parent bodies [e.g., *McSween*, 1989]; (2) solar system chronology [e.g., *Kleine et al.*, 2009]; (3) environments and processes within the presolar nebula [e.g., *Desch*, 2006; *Huss et al.*, 2003]; and (4) the interstellar medium and its precursor stellar/galactic source environments [e.g., *Timmes and Clayton*, 1996; *Zinner et al.*, 2006]. Meteorites that fall on Earth are not generally considered to provide information about the Earth beyond that of early solar system chronology (e.g., timing of core-mantle differentiation, accretion, etc.). However, meteorites on the surfaces of other solar system bodies have the potential to contribute information about a variety of topics of high scientific interest.

[7] As with all solar system bodies, Mars has continued to interact with the interplanetary medium since its formation. The arrival of nonindigenous materials evident by fresh meteoroid impacts continues to the present day [*Malin et al.*, 2006]. Any fragments of this material that are not vaporized upon hypervelocity impact will begin to alter in their new environment. Meteoroid survival as meteorites is increasingly likely for smaller bolide diameters. The utility of meteorites found on the surface of Mars for probing a variety of important Mars- and meteoroid-related problems has recently been recognized [*Ashley and Wright*, 2004; *Ashley and Velbel*, 2007; *Ashley et al.*, 2008; *Bland and Smith*, 2000; *Chappelow and Sharpton*, 2006b; *Chappelow and Golombek*, 2010a; *Fleischer et al.*, 2009, 2010a; *Johnson et al.*, 2009, 2010; *Landis*, 2009; *Nuding and Cohen*, 2009; *Schröder et al.*, 2008, 2009a, 2009b, 2010; *Squyres et al.*, 2009, 2010]. Mars-specific applications of meteorite-based science include (1) understanding extraterrestrial contributions to soils and sedimentary rocks [*Flynn and McKay*, 1990; *Yen et al.*, 2005a, 2006]; (2) helping to provide constraints on atmospheric density and fragmentation behavior [*Chappelow and Sharpton*, 2006a, 2006b; *Chappelow and Golombek*, 2010a, 2010b]; (3) improving our understanding of impact processes; and (4) potential assistance with habitability assessments [e.g., *Gronstal et al.*, 2009; *Yen et al.*, 2006]. One of the most direct applications of meteorites found on Mars is as control or 'witness' samples for probing both physical (mechanical/abrasive) and chemical weathering. The hypersensitivity of most meteorites to mineral-volatile interactions (see section 2.1.1) makes them particularly well suited to the latter purpose.

[8] The MER rovers' Athena science payloads were designed in part to evaluate the effects of water on Martian surfaces, and the search for these effects constitutes one of the main mission science objectives. The instrumentation includes two primary remote sensing detectors: the 5–29 μm wavelength Miniature Thermal Emission Spectrometer (Mini-TES) [*Christensen et al.*, 2003] and 432–1009 nm wavelength, 16-filter panoramic camera (Pancam) [*Bell et al.*, 2003]; as well as four tools on the Instrument Deployment Device (IDD) or rover 'arm,' including the Alpha Particle X-ray Spectrometer (APXS) [*Rieder et al.*, 2003], Mössbauer Spectrometer (MB) [*Klingelhöfer et al.*, 2003], 31 μm pixel^{-1} Microscopic Imager (MI) [*Herkenhoff et al.*, 2003], and Rock Abrasion Tool (RAT) [*Gorevan et al.*, 2003]. The rovers also carry navigational cameras (Navcams), and hazard assessment cameras (Hazcams) [*Maki et al.*, 2003]. Nearly all of these instruments are useful for meteorite identification and evaluation. Indeed, use of the full instrument suite is valuable for an accurate determination of meteorite type [*Schröder et al.*, 2008].

2.1. Meteorite Weathering in Arid Environments as It May Apply to Mars

[9] While strong evidence for water in Mars' ancient past appears in the form of outflow channels, valley networks, gullies, and hydrous minerals [e.g., *Bibring et al.*, 2005, 2006, 2007; *Carr*, 1996; *Carr and Head*, 2003; *Christensen*, 2003; *Horgan et al.*, 2009; *Mustard et al.*, 2008], the role(s) of water in liquid, vapor, and ice phases in more recent epochs is less well established. The lower availability of water during the Late Hesperian and Amazonian periods would almost certainly make hydrologic effects in these times more subtle. Most effects in recent times are likely to result from mineral-water interactions (chemical alteration) [e.g., *Wyatt et al.*, 2004]. Because of their sensitivity, the occurrence of meteorites at the planet's surface may provide a means to address even the most subtle of these alteration processes.

[10] Mars presents an ideal situation for preservation of the surviving (low velocity) fraction of meteoroid arrivals because of its low-temperature, arid conditions. The Meridiani plains are sometimes compared to meteorite collecting locales on Earth where the "signal to noise ratio" for meteorites is high because of the general paucity of loose surface rocks. As meteorites found at Antarctic blue ice stranding surfaces [e.g., *Harvey*, 2003] provide opportunities to observe mineral-water interactions at subzero temperatures in contact with water ice, it has been suggested that meteorite weathering scenarios in Antarctica may be

a.

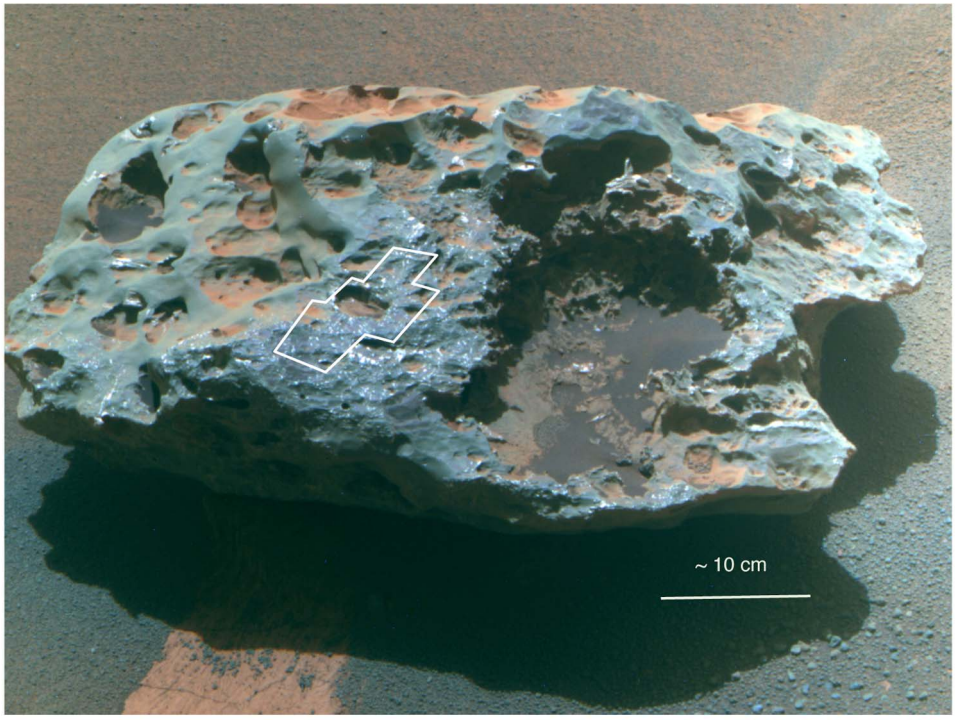

b.

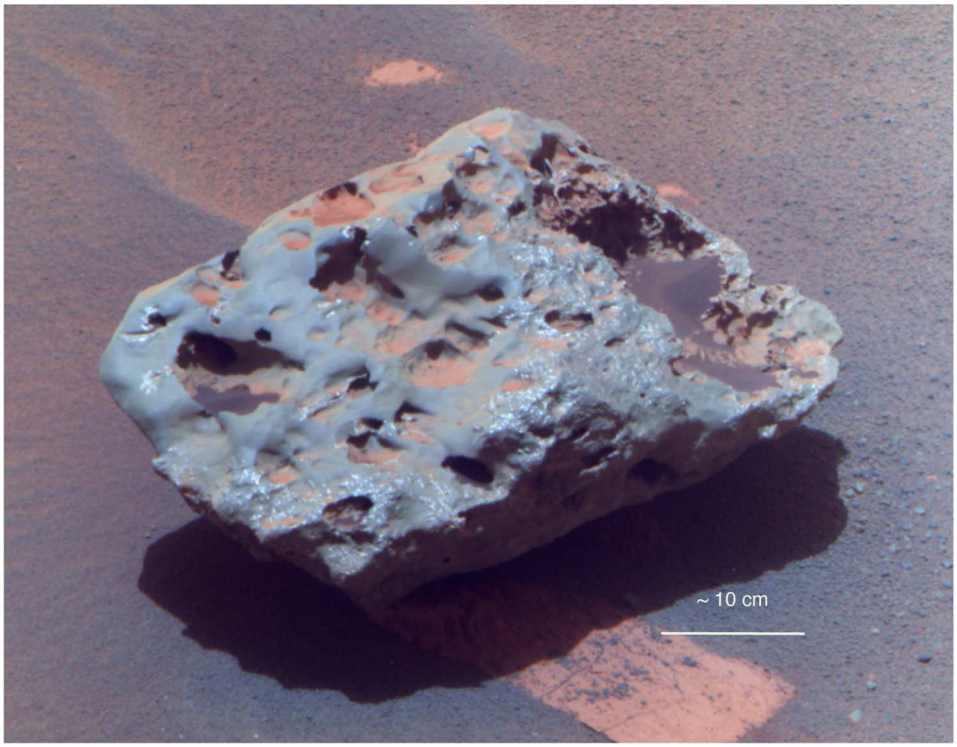

Figure 2

analogous to low-temperature "hydrocryogenic" alteration situations on Mars [*Gooding*, 1989; *Wentworth et al.*, 2005], with differences in pressure between the two worlds being negligible for these effects [*Gooding et al.*, 1992]. Also to be considered as potential analog locations are the typically drier (though significantly warmer) Roosevelt County, New Mexico, Australian, northwest African, and Saharan desert sites. While weathered meteorites collected from these sites may serve as a starting point for Martian studies, it must also be understood that exposure durations, temperatures and wetting frequencies for meteorites on Mars may vary significantly from those of Earth-based sites.

2.1.1. Metallic Iron Oxidation in Desert Meteorites

[11] Secondary (postfall) iron oxidation (i.e., weathering) has been studied in cold-desert, Antarctic meteorites [*Ashley and Velbel*, 1997, 2007; *Buchwald and Clarke*, 1989; *Gooding*, 1978, 1986b, 1989; *Velbel and Gooding*, 1990; *Velbel et al.*, 1991]; and in the hot-desert environments of Roosevelt County [*Bland et al.*, 1998a], New Mexico, Arizona, the Nullarbor Region of Western Australia, and the Algerian, Libyan, Saharan and Atacama deserts [*Bland et al.*, 1998b; *Muñoz et al.*, 2007]. Iron oxidation tends to be the predominant chemical process in the weathering of meteorites that contain metallic iron [e.g., *Gooding*, 1986b, *Bland et al.*, 2006] (which includes some 88% of all terrestrial falls [e.g., *Dodd*, 1981]). The metal content ranges from < 1% for LL ordinary chondrites [*Dodd*, 1981]; to more than 20% for H ordinary chondrites [*Pun et al.*, 1990]; as subequal volumes with silicate phases in the case of many stony irons and CB chondrites [*McCoy et al.*, 1990; *Weisberg et al.*, 2002]; and close to 100% for irons (minus sulfides, occasional silicates, graphite nodules, and other nonmetal fractions).

[12] Mössbauer analysis of ordinary chondrites indicates the presence of goethite (α-FeOOH), akaganéite (β-FeOOH; $Fe^{3+}{}_{15}Ni_{6.4}(OH)_{9.7}Cl_{1.3}$), and lepidocrocite ($\gamma$-FeOOH) oxyhydroxides, in addition to magnetite (Fe_3O_4) and maghemite (γ-Fe_2O_3) oxides, as common weathering products [*Bland et al.*, 1998b; *Muñoz et al.*, 2007]. Because their starting chemistries, mineralogies, and textures are well known, *Bland et al.* [1998b] suggest that ferric iron abundances within the bulk interiors of these samples are an index by which weathering intensities can be measured, and are therefore a gauge for climate history.

[13] Although rates of chemical weathering on Mars are significantly lower than those found on Earth [e.g., *Bland and Smith*, 2000], meteorites are nonetheless expected to be susceptible to alteration in many Martian environments. Meteorites in the equatorial regions of Mars have been estimated to decompose completely from chemical weathering on a 1 Ga time scale if they fell during a time when liquid water was available [*Bland and Smith*, 2000]. If we assume that many or most meteorites resting on the surface are likely to be more recent (Hesperian to Amazonian) additions to the planet, then their aqueous alteration would tend to address the effects of more recent (and therefore probably more subtle) water availability.

[14] Reduced iron metal should oxidize readily on Mars in the presence of even trace amounts of water, though secondary mineralogy may vary depending on the phase and abundance of that water. Qualitative chemical reactions illustrating spontaneous aqueous alteration tendencies on Mars are presented by *Gooding et al.* [1992], where water vapor interacting with the meteoritic sulfide mineral troilite, for example, is predicted to produce a hydrated iron sulfate. Such a result might be anticipated in the presence of high water vapor or acid fog [e.g., *Schiffman et al.*, 2006]. The formation of an oxyhydroxide mineral is thermodynamically preferred in the event of a liquid water interaction [*Gooding et al.*, 1992]. Well-crystallized products may include goethite, akaganéite, and lepidocrocite, where akaganéite sequesters its chlorine from the environment [*Buchwald and Clarke*, 1988, 1989], although this may be a metastable phase [e.g., *Bland et al.*, 2006]. The presence of the hydroxyl radical is accepted as evidence of water exposure [e.g., *Gooding et al.*, 1992]. The following terrestrial example for the formation of akaganéite from meteoritic iron metal in an oxidizing environment is borrowed from *Bland et al.* [2006], where the Cl^- ion has exchanged with the OH^- ion.

$$2Fe_i + O_2 + 2H_2O \xrightarrow{\text{irreversible}} 2Fe(OH) + 2OH^- \quad (1)$$

$$2Fe(OH) + 2OH^- + 0.5O_2 \xrightarrow{\text{irreversible}} 2\beta\text{-}Fe^{3+}OOH + H_2O \quad (2)$$

Even when oxygen is entirely lacking as a volatile, the oxygen atom in the water molecule should be sufficient to oxidize ferrous iron in olivine on Mars (M. Zolotov, personal communication, 2007). Because olivine alteration is less spontaneous than metallic iron (Fe°) oxidation [e.g., *Bland et al.*, 2006], meteoritic iron-nickel metal is likely to be the most sensitive material to aqueous alteration on the surface of Mars. Much of the granular iron in chondritic meteorite matrices is found within the cryptocrystalline size fraction, magnifying the alteration susceptibility by increased surface area:volume ratios [e.g., *Burns and Martinez*, 1991]. Therefore, spontaneous oxidation should be the case unless the meteorite is somehow preserved in a reducing environment, [e.g., *Birch and Samuels*, 2003].

Figure 2. False color Pancam images presenting three views of the Block Island meteorite: (a) north facing, (b) east facing, and (c) south facing surfaces. White outline in Figure 2a shows the overlay of the New Shoreham Microscopic Imager (MI) mosaic (presented as Figures 4a–4c). (d) Gray scale Navcam image illustrates the surface roughness dichotomy: smooth and worn to the south (right) of the red line, and angular and craggy to the north (left) of the red line. The meteorite was estimated at approximately 60 × 40 × 25 cm in size based on Navcam image measurements [*Chappelow and Golombek*, 2010b]. (e) A three-dimensional geometric model of Block Island, showing approximate north, south, east, and west sides in images starting from the top left and continuing clockwise. The model was used to calculate a volume estimate of 30,429 cm^3. Assuming a uniform density of 7.9 g cm^{-3} (kamacite density) gives a mass of 240 kg for the meteorite. The model was prepared by JPL's Multimission Image Processing Laboratory using Pancam and Navcam images taken from six ~1 m standoff positions. Image credits: NASA/JPL/Pancam/MIPL.

c.

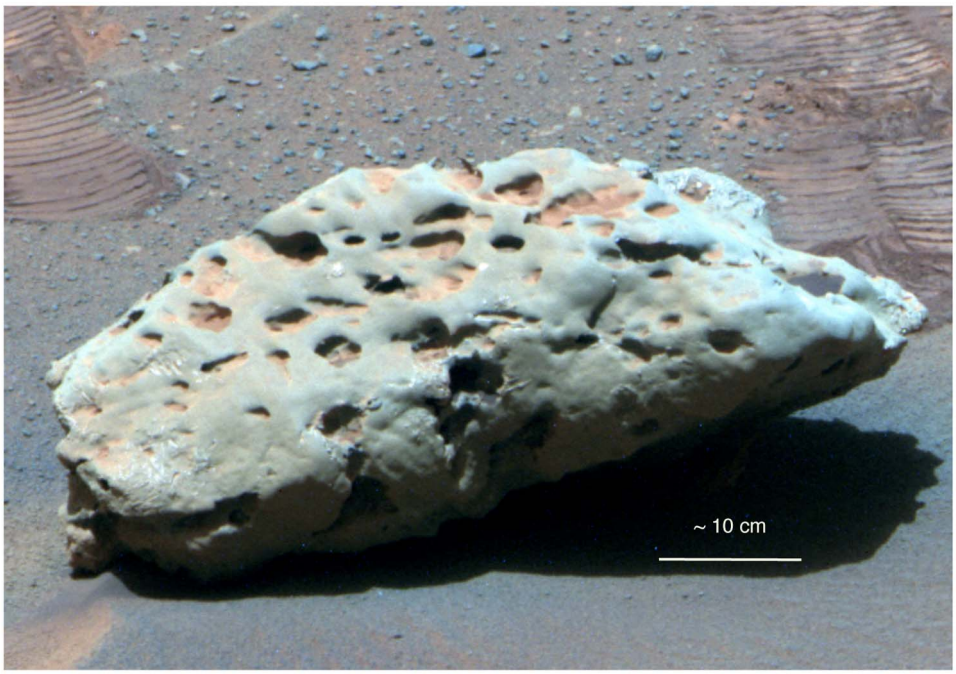

d.

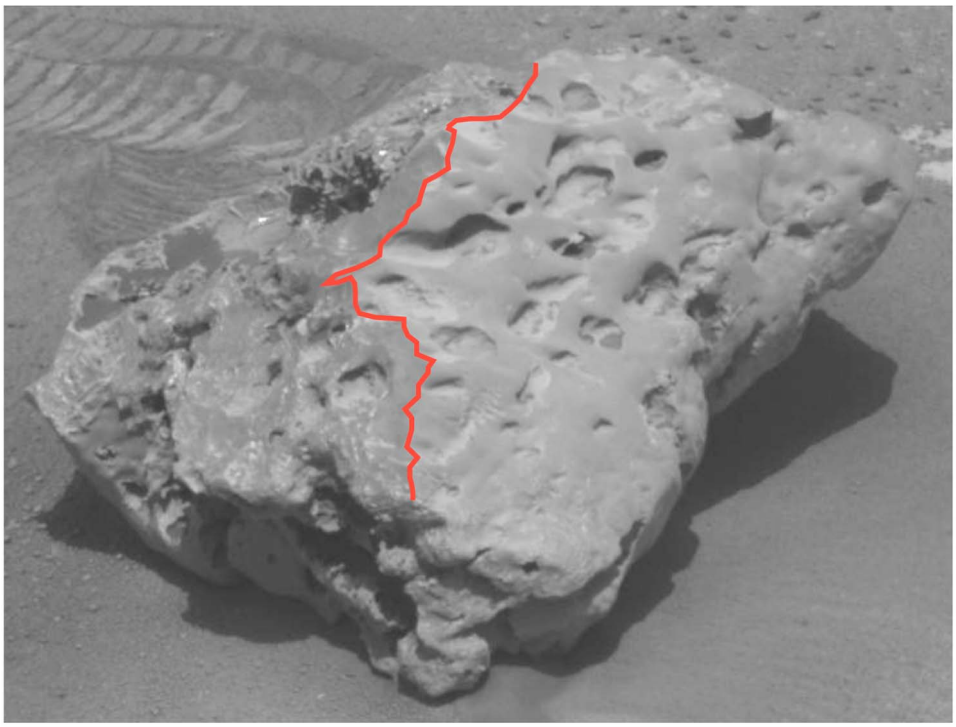

Figure 2. (continued)

2.1.2. Meteorite-Water Interactions at Subzero Temperatures and Ice Occurrence on Mars

[15] Water ice is almost certainly more available for surface-volatile interactions than liquid water in the modern Martian epoch [*Wyatt and McSween*, 2006]. Monomolecular films of liquid water can exist on mineral grain surfaces at subzero temperatures in Antarctic meteorites [*Gooding*, 1986a; *Velbel and Gooding*, 1990]. Such films can facili-

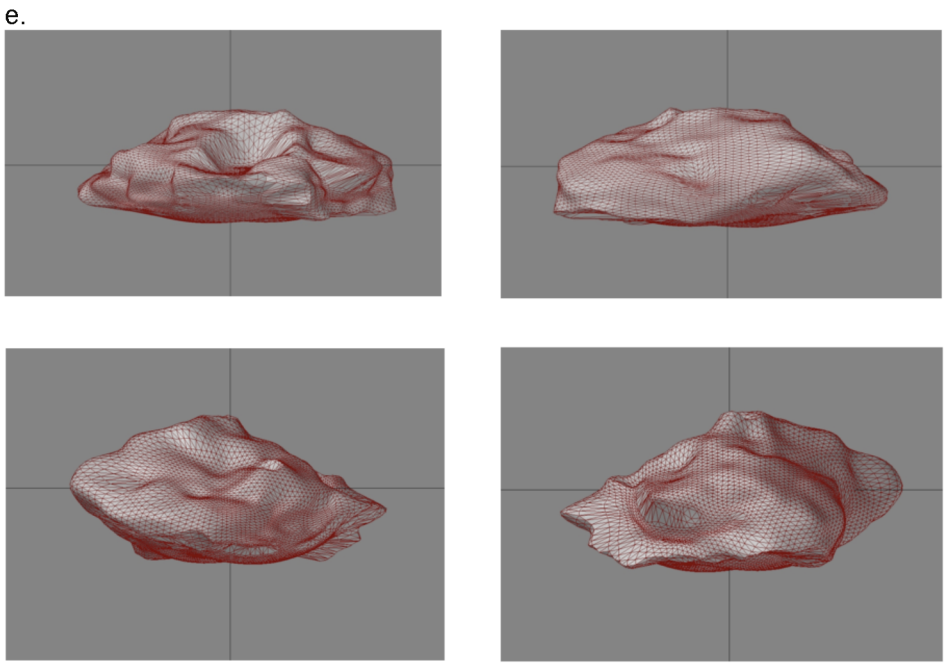

Figure 2. (continued)

tate the elemental migration necessary for many alteration reactions. Antarctic stony meteorites exposed to sunlight may have internal temperatures (at depths up to 2 cm in some meteorites) as high as 5°C on wind-free days (even when air temperatures remain below 0°C), enabling capillary waters to promote reactions [*Schultz*, 1986b]. Significantly, some iron oxidation reactions have been found to occur in the solid state at low relative humidities [*Buchwald and Clarke*, 1989]. Aqueous processes are active in permanently frozen Antarctic soils [e.g., *Campbell and Claridge*, 1987]. The shallowest ground ice on Mars is likely to be in diffusive equilibrium with the atmosphere [*Mellon et al.*, 2004], and *Yen et al.* [2005b] found that multimonolayer films of water within the shallow subsurface at Gusev crater (~15°S) were likely to promote rock weathering under current obliquity conditions. Observations of water frost on the Opportunity rover (<2° S) during late southern winter demonstrates that unstable water ice can reach equatorial regions in periods of low obliquity [*Landis*, 2007].

[16] The latitudinal extent of *stable* ground ice on Mars is debatable, though it is generally not considered stable at the current obliquity within 45° of the equator unless it is protected by a layer of low-permeability material [*Mellon et al.*, 2004], in which case it may be present near the equator at relatively shallow depths [*Feldman et al.*, 2004]. However, surficial water ice may have been stable at significantly lower latitudes (and perhaps even within equatorial regions) during periods of high obliquity on time scales of 50,000 yr to 2 Ma [*Mellon et al.*, 1997]. Other models indicate that near-equatorial latitudes may have been ice free by 2.7 Ma [*Mischna et al.*, 2003]. At an obliquity of 32°, ground ice becomes stable globally, and at 45° obliquity, only the equatorial regions would have been able to sustain it [*Mellon and Jakosky*, 1995]. Oxide/oxyhydroxide coatings identified on Martian finds in near-equatorial latitudes (where both MER vehicles are located) are therefore likely to result from subzero monolayer or multilayer water interactions within the shallow subsurface under obliquity conditions similar to the present one, with enhancement during periods of higher obliquity.

2.2. Operational Approaches to Meteorite Identification and Reconnaissance

[17] Meridiani Planum is characterized by unconsolidated, windblown basaltic sand discontinuously overlying a sulfate-rich sandstone bedrock containing hematite "blueberry" concretions [e.g., *Squyres et al.*, 2004]. An absence of Hesperian age craters, thermal inertia and spectral evidence, and hematite blueberry lag concentration values for the area suggest that the region has undergone up to 10–80 m of deflation within the past 3 Ga, resulting in a level and nearly rock-free surface [e.g., *Christensen and Ruff*, 2004; *Golombek et al.*, 2006]. Evidence for ancient acidic groundwater [e.g., *Grotzinger et al.*, 2006, 2005; *McLennan et al.*, 2005; *Squyres et al.*, 2004; *Tosca et al.*, 2005; *Zolotov and Shock*, 2005] indicates that environmental conditions in the distant past were dramatically different from those today.

[18] As Opportunity traverses across the Meridiani plains, images are acquired at the end of each drive for traverse planning. Typical end-of-drive coverage is a 3 × 1 stereo Navcam mosaic and a 4 × 1 stereo Pancam in either red or blue filters depending on the terrain, both pointed in the intended drive direction. These images provide the minimum information required for planning the next drive, but they are not ideal for searching for meteorites. So when data volume restrictions allow, traverse planning images are augmented by expanding the Navcam coverage (often to complete a full 360° panorama), and adding one or more

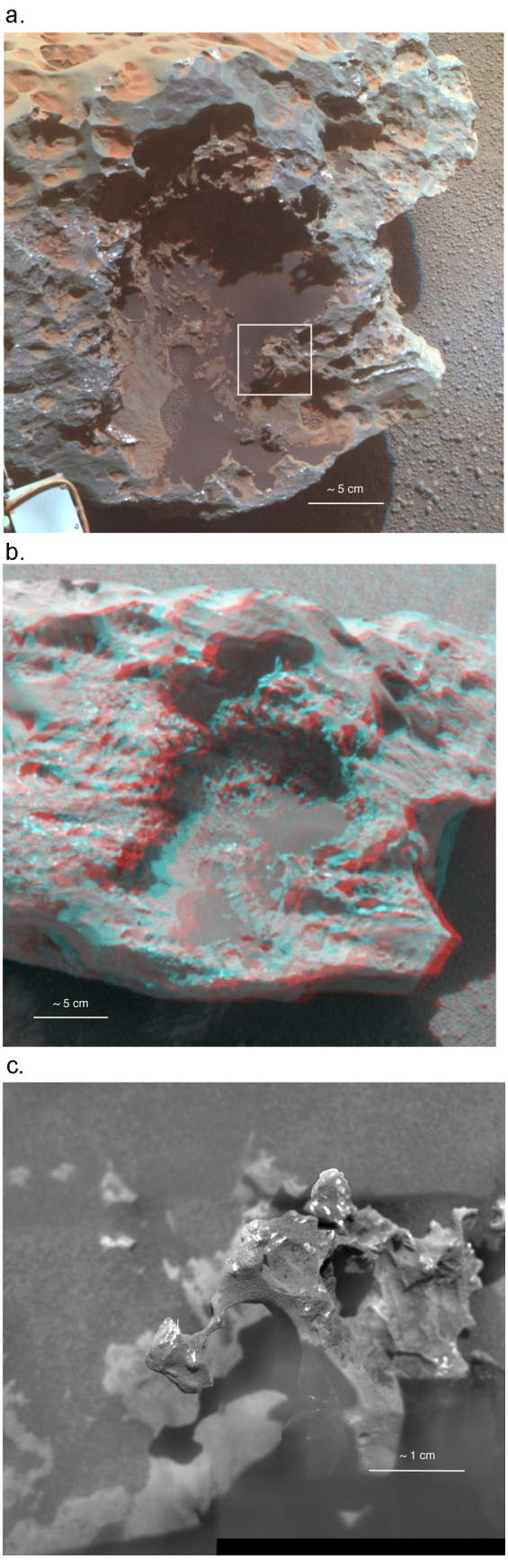

filters to the Pancam coverage to provide improved color discrimination.

[19] Prospective meteorites are identified in such coverage based on their size, albedo, and (in some cases) color contrast with typical Meridiani bedrock. Because blocks of Meridiani sandstone erode away so quickly, rocks of a size large enough to be apparent in such coverage are often meteorites. Images showing meteorite candidates may be downlinked after the rover has moved on from the location where the images were acquired, requiring a decision to backtrack if the prospective meteorite is going to be investigated. Depending on its initial distance from the rover when noticed, its azimuth from the planned drive direction, and its perceived degree of potential science value, a candidate meteorite may be approached for closer inspection. Different levels of analysis may then be employed (i.e., remote sensing versus full instrument deployment), again depending on the perceived science potential.

[20] Several different cobble groups have now been identified by Opportunity at Meridiani Planum by these methods [*Fleischer et al.*, 2010b], and meteorites comprise a significant fraction of them. Each of the following meteorites displays its own set of morphologic characteristics, with each providing clues to one or more of the processes in operation at Meridiani Planum over time.

3. Iron Meteorite Descriptions

3.1. Block Island

[21] Opportunity arrived at Block Island on sol 1961, 4.2 km along its approximately 12 km traverse toward Endeavor from Victoria crater. In broad outline, the iron-nickel rock appears somewhat pillow or trapezoidal shaped, with rounded upper and lower surfaces, and appears to rest as a protective "caprock" on a partially eroded 4 cm high pedestal (similar to a hoodoo) (Figures 2a, 2b, and 2c). The largest meteorite yet identified on Mars, it is approximately 60 cm across its long axis, with a calculated mass of ~240 kg (assuming a typical iron meteorite density of ~7.9 g cm^{-3}) [*Chappelow and Golombek*, 2010b]. It has many rounded hollows, with several of the lower hollows (within 15 cm of the ground) containing loose hematite blueberry concretions and sand.

[22] Block Island displays a distinct dichotomy in its surface roughness (Figure 2d). Approximately 75 percent of its exposed surface, including the south facing portion, is rounded with smooth outlines to the hollows. The remaining quarter of the exposed upper surface and its western

Figure 3. (a) False color Pancam image of cavernous pit in Block Island. Note highly angular, relic metal protuberances along the rim and shelf-like features near the north lip (toward the bottom in the image). (b) The anaglyph presents better illumination of the cavern interior, showing coarser texture than found in more exposed portions of the pit. Angularity and hardness of metal skeletons precluded IDD use within the pit. White rectangle in Figure 3a shows (c) MI target named Veterans Park: a metal skeleton structure relic after some alteration process has removed less resistant material, collected on sol 1979 (note shadow for relief). Image credits: NASA/JPL/Pancam.

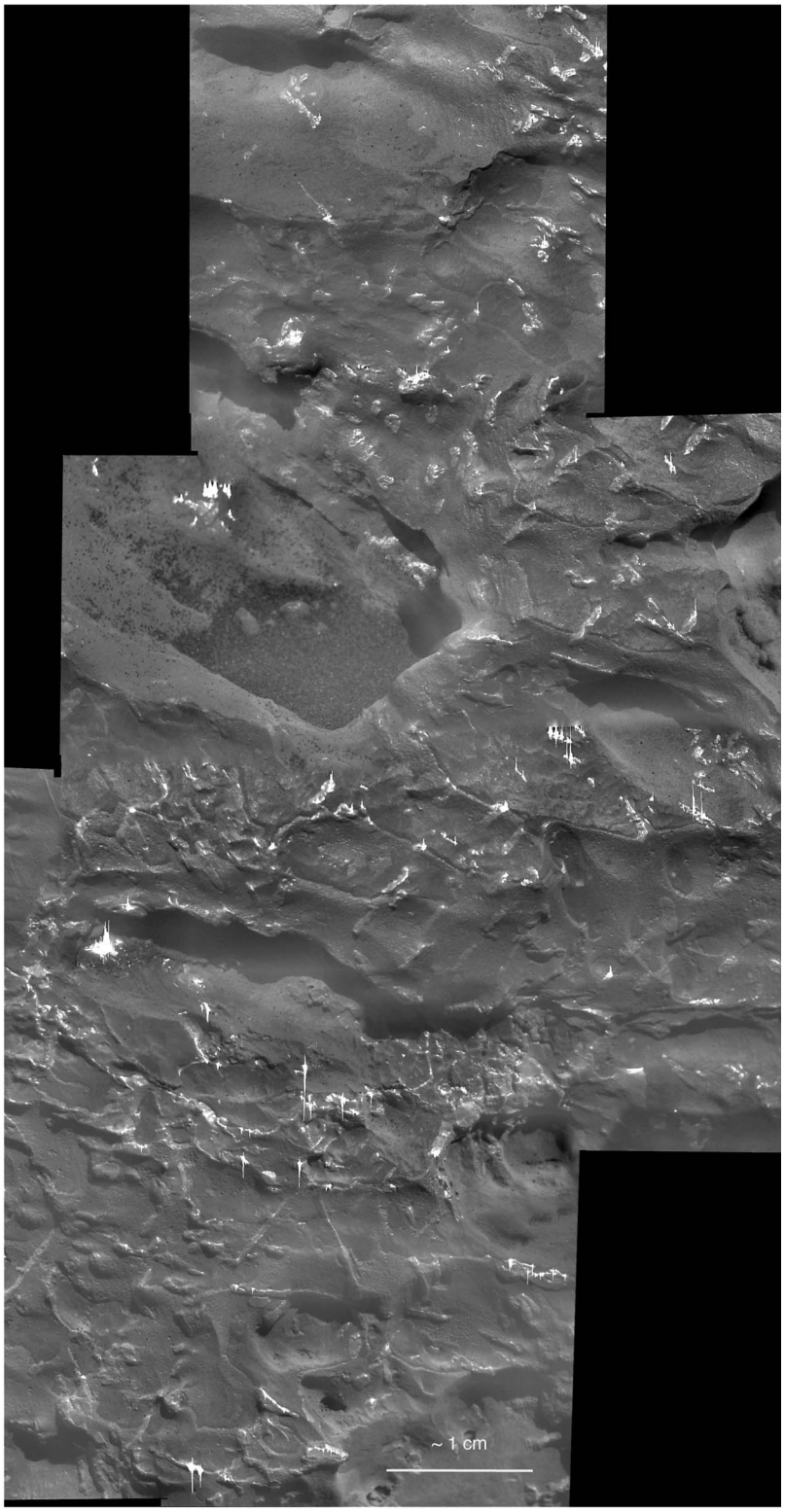

Figure 4

undersurface are significantly more rough and angular in their features, and display specular reflections in Pancam images not seen on the rounded portions. The hollows within this latter surface appear more angular in outline than those on the smoother surfaces. The smoother portion also appears to be more heavily dust-coated, based on Pancam color images (Figure 2c).

[23] Also within the rougher, northern side of the meteorite, and perhaps more significantly, Block Island presents a large (~20 cm long dimension), cavernous pit (Figures 3a and 3b). The pit is roughly elliptical in outline, and coalesces with a number of smaller pits near the apex of the rock. It is also rimmed by an irregular network of relic metal protuberances or "skeletons," and shelf-like structures. Some of these features appear remarkably fragile (Figure 3c).

[24] MI images taken within the rough portion of the surface show clear indications of a differentially eroded Widmanstätten pattern (common to several classes of iron and stony iron meteorites; refer to section 4 for a discussion). A discontinuous, dark-toned coating is also present across much of the meteorite's surface (Figures 4a, 4b, and 4c). The coating is similar to that noted on Heat Shield Rock [*Schröder et al.*, 2008; *Johnson et al.*, 2010] (located 9.6 km to the north of Block Island). The full IDD instrument suite was employed at several target areas over a nearly 6 week period on Block Island, and Pancam/Navcam coverage from six locations around the meteorite was acquired prior to departure. This coverage allowed Multmission Image Processing Laboratory (MIPL) of JPL's Interplanetary Network Directorate to render a three-dimensional model of Block Island (Figure 2e), which was used to estimate the meteorite's mass.

3.2. Shelter Island

[25] Figures 5a and 5b present false color Pancam images of Shelter Island, first encountered on Sol 2022. It has a long dimension of ~52 cm, and has a mass of ~100 kg [*Chappelow and Golombek*, 2010b]. By contrast with Block Island, this rock does not show particularly distinct variations in surface roughness. However, one of the hollows contains a mass of unknown mineralogy (but which might be a kamacite plate or taenite lamella) that appears to be weathering out of its groundmass (red arrow in Figures 5a and 5c). It also exhibits large-scale excavations penetrating deeper into its interior near its base than observed in Block Island. This meteorite appears generally more weathered than Block Island, with spires of residual metal resulting from extensive erosion along a northeast-southwest axis (Figure 5b). Other portions of the rock appear relatively fresh with smooth surfaces and hollows that were likely formed as a result of ablation during atmospheric entry. Pancam and Navcam images were collected from three circumferentially spaced standoff (and two additional) positions, together with IDD instrument placement on one surface target location named Dering Harbour. As with Block Island and Heat Shield Rock, Shelter Island presents differentially eroded Widmanstätten lamellae and a dark, surficial coating. This coating, however, appears somewhat more continuous in the target area than was seen on Block Island. Most of the hollows on this rock contain sand and blueberries, including those near the top.

3.3. Mackinac Island

[26] This meteorite, encountered on sol 2034, is the smallest of the three at 30 cm in diameter (comparable to Heat Shield Rock), and has a hemispherical mass of ~65 kg based on its triaxial ellipsoidal measurements and assumed density [*Chappelow and Golombek*, 2010b] (Figures 6a and 6b). The rock exhibits an even more severe example of mass removal, showing an excavated interior, similar to cavernous weathering, along a southeast–northwest axis (likely significantly reducing its calculated mass), with a metal lacework all that remains of the former mass in some regions (Figure 6b). Portions of Mackinac Island are smooth with rounded hollows. Like the other meteorites, blueberry concretions and sand are often found within these hollows. Mackinac Island was imaged by Pancam from three standoff positions, one of which included 13-filter images, but was not investigated using any IDD instruments.

4. Interpretations and Discussion

[27] The surfaces of freshly fallen meteorites on Earth typically exhibit regmaglypts and fusion crusts. Regmaglypts are morphologic features resulting from ablation at high temperature during atmospheric entry, often described as resembling "thumbprints." They vary in size from < 1 cm to several cm from interactions with turbulent, supersonic airstreams, and tend to form in coherent sets or patches with wave-like "crest and trough" topography [*Buchwald*, 1975] (Figure 7). Block Island MI mosaics confirm the presence of regmaglypts within the Meridiani iron suite (ellipse in

Figure 4. (a) Sol 1963 MI mosaic of New Shoreham IDD target region surface texture; location shown in Figure 2a overlay. The images demonstrate the presence of the Widmanstätten pattern common to iron-nickel meteorites (most notably in lower third, but present throughout image area). Taenite lamellae are characterized by lighter, linear zones, frequently with specular reflections, often casting shadows showing that they are topographically higher than the surrounding surfaces. The intergrowth of the kamacite and taenite crystal structures produce different patterns when sectioned at different angles. (b) The three taenite lamellae forming nearly perfect 60° intersections (enlarged in Figure 4b) provide the orientation of the immediate surface of the meteorite with respect to a local kamacite/taenite octahedron; central image in schematic inset. The differential erosion of this pattern demonstrates a form of mechanical (aolian abrasion) weathering. The ellipse in Figure 4b highlights a classic regmaglypt. The regmaglypt to its immediate left (not outlined) has been modified postfall and is undercutting a taenite lamella. (c) Discontinuous coating patches (darker gray zones) are seen as residual deposits between and marginal to kamacite plates and within topographic low areas below the height of these erosional features, implying that they were deposited after erosion and therefore represent something other than fusion crust: most probably a weathering rind produced by water interaction in a subsurface situation. Compare with Figure 13. Image credits: NASA/JPL/MI.

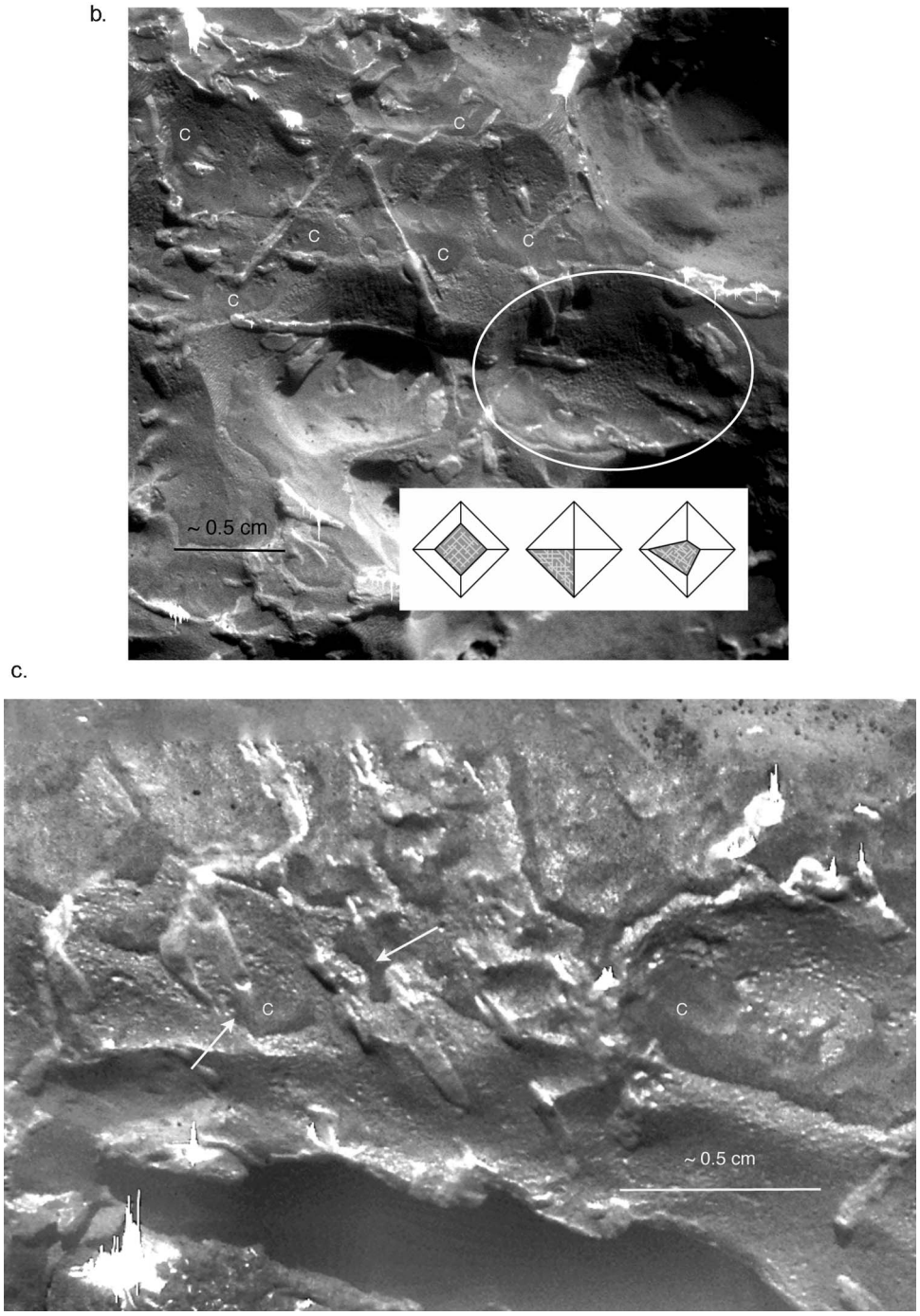

Figure 4. (continued)

Figure 4b). Further, all of the Meridiani meteorites feature smooth-shaped hollows that are either regmaglypts or slightly modified regmaglypts. Other instances of cavity enlargement may be regmaglypt controlled in their spacing, but may also be caused by the removal of troilite nodules, which (if pure) can excavate completely during atmospheric entry [*Buchwald*, 1975]. In each case, enough of the atmospheric interaction imprint remains to conclude that portions of these meteorites have not changed significantly from their original postfall outlines.

[28] Fusion crusts also result from frictional interactions with the atmosphere during entry [e.g., *Norton*, 2002]. They vary in thickness (typically < 1–2 mm) and composition, but tend to be similar in composition to their substrates. Iron meteorite fusion crusts may be composed of alternating magnetite-rich and metal sheets [*El Goresy and Fechtig*, 1967], and may appear ropey with a heat-affected zone just beneath the crust evident in cross section [*Buchwald*, 1975].

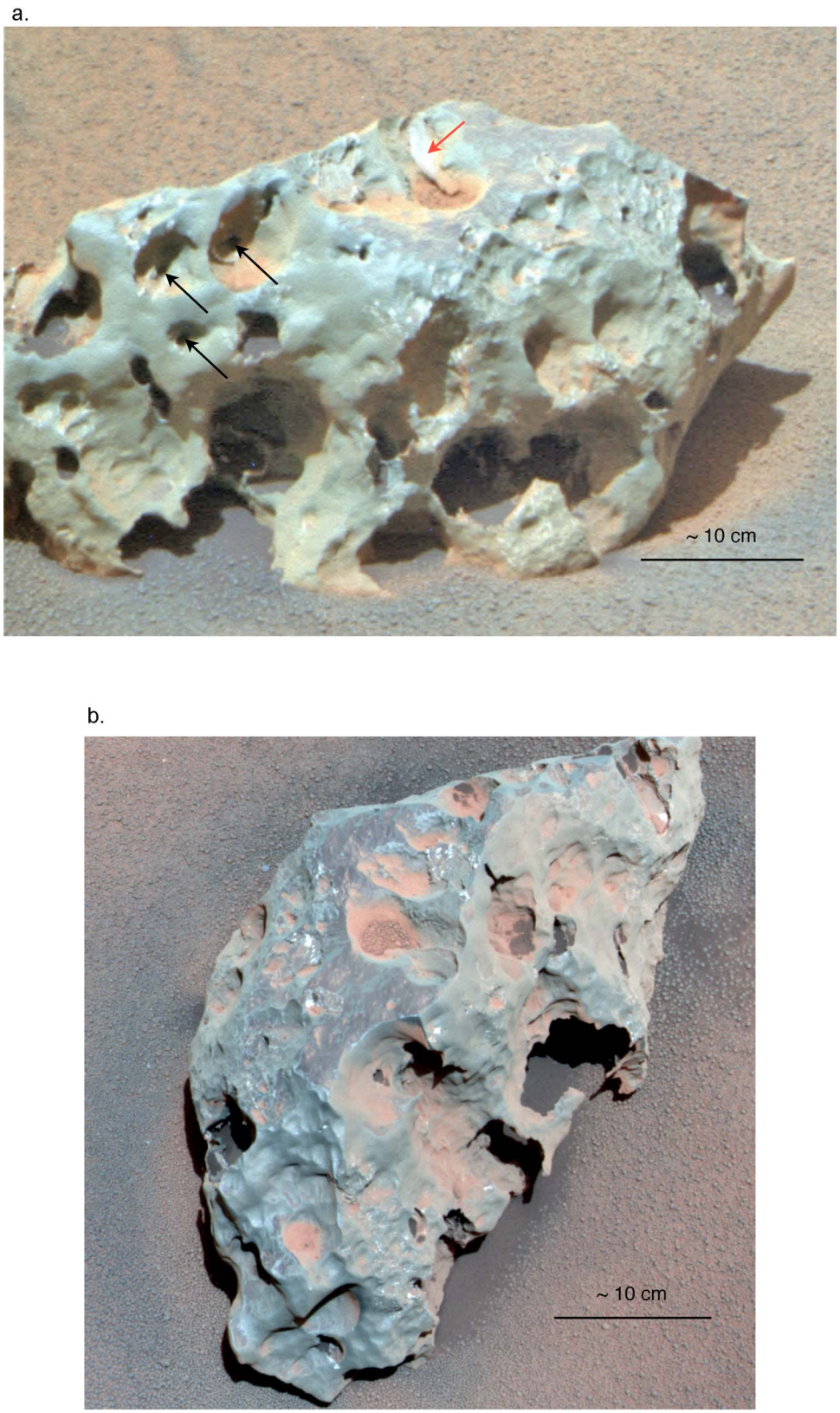

Figure 5

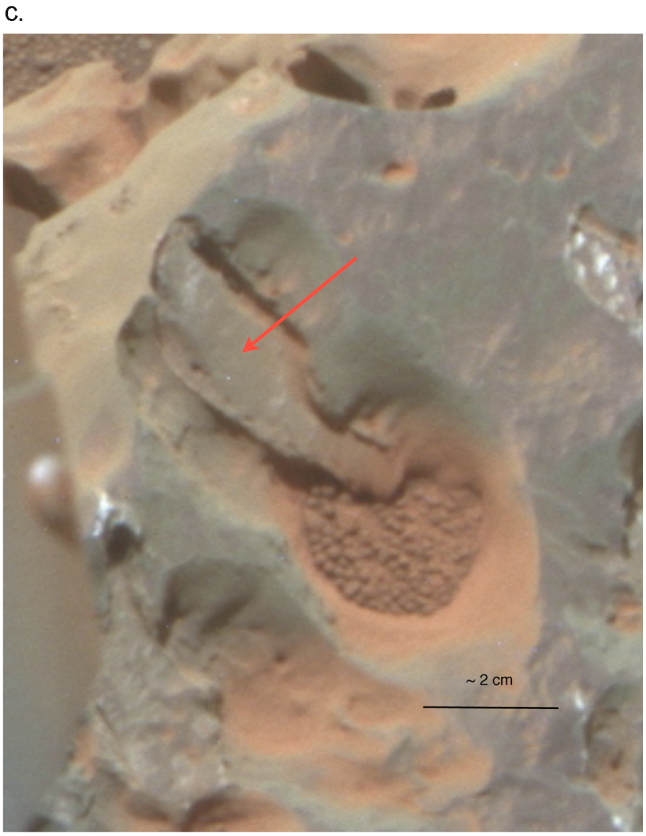

Figure 5. (continued)

[29] In order for meteorites to be effective witness samples for weathering processes, it is necessary to distinguish regmaglypts and fusion crusts (both features formed by atmospheric interactions) from features produced by alteration of the rock's surface after it arrived on the ground. Therefore an objective for the Meridiani iron suite is to separate three classes of surface modification: (1) atmospheric ablation, (2) aqueous alteration, and (3) eolian modification. This is not always straightforward, even for meteorites found on Earth. Further, many of the surface features discussed for the Meridiani iron suite are likely to be the result of more than one of these processes. For example, evidence for both mechanical and chemical weathering processes has been noted in Heat Shield Rock [*Ashley et al.*, 2009a; *Fleischer et al.*, 2010a; *Schröder et al.*, 2008], but some conclusions have remained ambiguous.

[30] New data collected for Block Island, Shelter Island, and Mackinac Island augment our understanding of weathering processes for Meridiani Planum iron meteorites, and provide clues sufficient to resolve some of the questions raised during Heat Shield Rock analysis. The following discussions are presented as a sequence of separate but interrelated problems that are addressed by these findings.

4.1. Significance of Cavernous Pit in Block Island

[31] The large cavernous pit on Block Island appears unique among the features observed in the Meridiani iron suite. Based on size alone, such a cavity might conceivably result from a fracture at the boundary between a pair of large taenite crystals (sometimes called austenite). Enlargement of such fractures to the size range of Block Island's pit is not uncommon during aqueous alteration of iron meteorites on Earth [e.g., *Buchwald*, 1975]. Large hollows can also sometimes form from atmospheric ablation. However, the pit morphology suggests that other processes are responsible. Regions along the pit margin preserve relic metal protrusions and delicate "filigree" structures unlikely to have survived atmospheric ablation (Figures 3a and 3b). An MI mosaic of the IDD target area on Block Island named Veterans Park shows one of the delicate metal protrusions

Figure 5. (a and b) False color Pancam images of Shelter Island meteorite. Noteworthy are the dramatic effects of mass removal processes, which seem to strongly prefer excavation of some volumes over others left almost unmodified. The phenomenon may be controlled partly by the occurrence of inclusions common to iron meteorites and partly by original regmaglypt locations. (c) Red arrow denotes a probable kamacite plate or taenite lamella weathering out of its groundmass, also shown at higher resolution. Black arrows denote depressions with small-diameter cavities at the base of each recess, producing a funnel-shaped cross section for the depression. Figure 5a has been enhanced to minimize shadow effects unavoidable at the time of imaging. Image credits: NASA/JPL/Pancam.

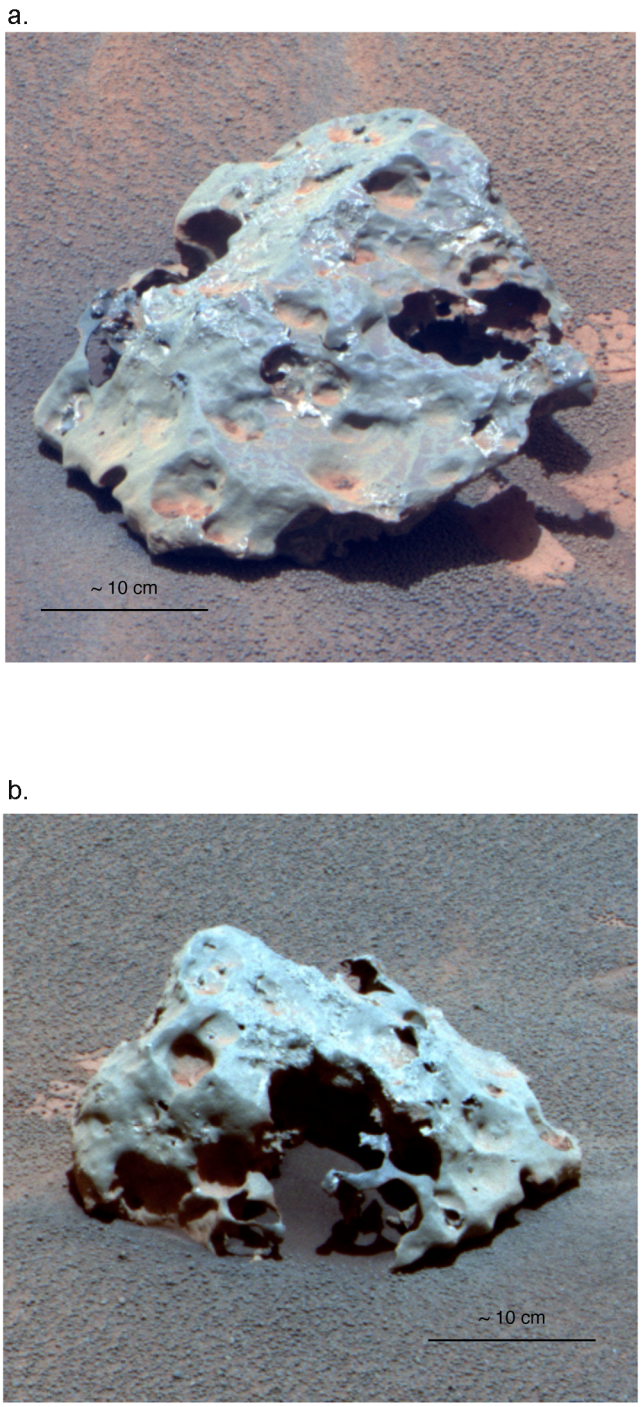

Figure 6. (a and b) False color Pancam images of Mackinac Island. This meteorite is so severely weathered that a significant fraction of its lower volume has been removed from its interior, leaving a webwork of residual metal behind. Shadows provide relief and demonstrate undercut nature of overhanging lower portion. Image credits: NASA/JPL/Pancam.

lining the rim of the pit (Figure 3c). These protrusions suggest that (1) a mass once present has been removed and (2) a corrosive process may have been partly responsible for the removal. No remnants of the former mass either within or around the pit are obvious in Pancam, Navcam or MI images. Surfaces within the pit range in angularity from rounded to highly angular. The more rounded surfaces are likely to have been modified by mechanical abrasion.

[32] Iron-nickel and pallasite meteorites are both known for containing several types of inclusions. Among these are large (several cm diameter) troilite and graphite nodules [e.g., *Coey et al.*, 2002; *Buchwald*, 1975], shreibersite and cohenite [e.g., *Fleischer et al.*, 2010c; *Birch and Samuels*, 2003] in irons, and the characteristic olivine phenocrysts of pallasite meteorites [e.g., *Mittlefehdt*, 1980]. Most terrestrial pallasites show a fairly uniform distribution of phenocrysts throughout their volume. Examples of strongly heterogeneous pallasites exist, however (e.g., the Seymchan pallasite [*van Niekerk et al.*, 2007]), as do examples of relic metal skeletons in pallasites attributed to weathering (e.g., Imilac [*Buchwald*, 1973] and Springwater [*Nininger*, 1932]). An example of Imilac is presented as Figure 8. Some pallasites exhibit metal protrusions similar to those of Block Island that almost certainly formed as a result of olivine grain plucking from the metal matrix during atmospheric entry. However, no residual olivine grains have been observed in Block Island, which would be expected for even a highly weathered pallasite. More importantly, Ga and Ge abundances measured for Block Island by APXS (R. Gellert, personal communication, 2010) are inconsistent with a pallasite interpretation.

[33] Based on the morphology, the cavernous pit in Block Island is most likely the result of a slow corrosion process (probably acidic), which would have occurred at some time after the meteorite's landing at Meridiani Planum. Although it is generally understood that the hematite-bearing sulfate bedrock at Meridiani reflects an acidic depositional environment [e.g., *Baldridge and Calvin*, 2004; *Squyres et al.*, 2004; *Zolotov and Shock*, 2005; *Hurowitz et al.*, 2010], these iron meteorites are likely to have fallen long after the sulfate bedrock was in place. Any corrosive process resulting in Block Island's cavernous pit would therefore require a

Figure 7. Example of unweathered, regmaglypted iron meteorite surface texture for reference purposes. Sikhote-Alin, observed to fall on 12 February 1947 in Sikhote-Alin mountains, Russia.

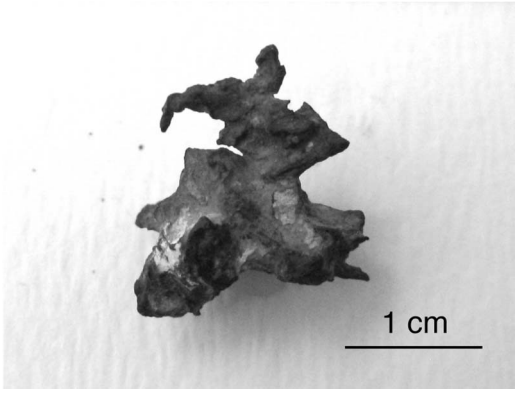

Figure 8. A fragment of the Imilac pallasite exhibiting similar metal skeletons on a similar scale to those found bordering the Block Island cavern pit. These features are attributed to postfall alteration and removal of olivine phenocrysts [e.g., *Buchwald*, 1973].

different type of mechanism, possibly involving thin films of water made acidic by interactions with meteorite inclusions or the bedrock itself. Further study is needed to determine a reasonable process, and other mass removal mechanisms cannot be ruled out at this time.

[34] The Block Island "filigree" structures are smaller than the metal spires seen in Shelter Island or Mackinac Island, and may therefore indicate a different type of removed mass than may have been present in these latter meteorites. The relic metal spires, protrusions and cavernous weathering features observed in Shelter Island and Mackinac Island may have a similar origin, but they could also be the result of protracted eolian erosion (discussed in section 4.3).

4.2. Fusion Crust Versus Secondary Coating

[35] While no obvious iron oxide or oxyhydroxide features are visible in the Mini-TES spectra for Heat Shield Rock [*Ashley et al.*, 2008], portions of its brushed surface show a dark (purple hued in false color Pancam composites and decorrelation stretches using 432 nm, 535 nm, and 753 nm filters [e.g., *Johnson et al.*, 2010; *Farrand et al.*, 2007]) and discontinuous coating interpreted to contain iron oxides/oxyhydroxides based on Mössbauer and APXS measurements [*Schröder et al.*, 2008], and on multifilter Pancam image analysis [*Johnson et al.*, 2010]. Figures 9a and 9b present Heat Shield Rock and a MI mosaic of an IDD target area showing a magnified view of this material and surrounding dust-coated surface. Approximately 5% of the iron at this location on Heat Shield Rock was measured to be in a ferric state, and some of that may be nanophase hematite [*Fleischer et al.*, 2010a]. However, distinguishing iron oxides from hydroxyl-bearing (and therefore water-indicative) oxyhydroxides is difficult. It is therefore unclear whether the dark coating on Heat Shield Rock is relic fusion crust, weathering rind, or possibly even a thin layer of welded particulates [*Schröder et al.*, 2008].

[36] The Block Island and Shelter Island meteorites also exhibit dark coatings similar in hue [*Johnson et al.*, 2009], composition [*Fleischer et al.*, 2010b], and occurrence to that found on Heat Shield Rock. Figures 4a, 4b, and 4c show an MI mosaic of an area of Block Island named New Shoreham, displaying the heterogeneous distribution of the coating. APXS-measured abundances of Mg and Zn in the Block Island coating were elevated relative to the uncoated surface (R. Gellert, personal communication, 2010). Figures 4b and 4c exhibit crosscutting relationships (embayments and topographic differences) between coating features and others interpreted to be the result of differential eolian abrasion (discussed in more detail in section 4.3). These relationships show the coating formed postfall, rendering a fusion crust theory unlikely and favoring a weathering product interpretation instead. This conclusion is supported by the discordant Mg and Zn chemistry between the coating and its substrate, which tend to be chemically similar in the case of true fusion crusts.

4.3. Atmospheric Ablation Versus Mechanical Abrasion

[37] The MI mosaic of Heat Shield Rock shows millimeter-sized chevrons and subparallel grooves, most prominent on a partially brushed surface approximately 3 × 2 cm in area (see Figure 9b). Other portions of the surface (including the dark coating discussed in section 4.2) appear to have been sculpted, locally forming ridges and cavity modifications. An interpretation of the chevrons and grooves is fairly straightforward. Similar patterns are observed on a number of hot- and cold-desert iron meteorites (e.g., Drum Mountains and Fort Stockton; Figures 10a and 10b, respectively), and are attributed to physical ablation by windblown sand grains (not dust [*Laity and Bridges*, 2009]) differentially weathering the kamacite (α-(Fe, Ni)) and taenite (γ-(Fe, Ni)) lamellae within the rock. This is an expression of the Widmanstätten pattern common to sliced, polished, and acid-etched surfaces of many iron-nickel meteorites with appropriate nickel composition [e.g., *Buchwald*, 1977]. The intergrowth of the kamacite (body-centered cubic) and taenite (face-centered cubic) crystal structures produce different patterns when sectioned at different angles.

[38] The MI mosaic of an area of Block Island named New Shoreham (Figures 4a and 4b) also shows dramatic evidence for exposure of the Widmanstätten pattern from differential erosion. One cluster of plates has a triangular arrangement (Figure 4b), a common feature of the Widmanstätten pattern seen in cut and etched iron meteorites. The equilateral shape of the triangle means that at least this small portion of the meteorite's surface is oriented nearly parallel to an octahedron face in the local crystal structure (see Figure 4b inset). Widmanstätten features are also found in Shelter Island MI images. The presence of a Widmanstätten pattern in Heat Shield Rock, Block Island, and Shelter Island is consistent with the nickel abundance identified by APXS measurements for these meteorites [*Fleischer et al.*, 2010b]

[39] While a regmaglypt interpretation for the smaller hollows in the Meridiani iron suite is warranted in many instances, differential weathering of softer sulfide (troilite) nodules or other inclusions in the metal groundmass may be responsible for further modification. An example of hollow formation or modification from mechanical abrasion is evident in Shelter Island where a mass of unknown mineralogy (likely a kamacite plate or taenite lamella) is weathering out of its groundmass (red arrow in Figure 5c). Because this type of feature does not result from atmospheric

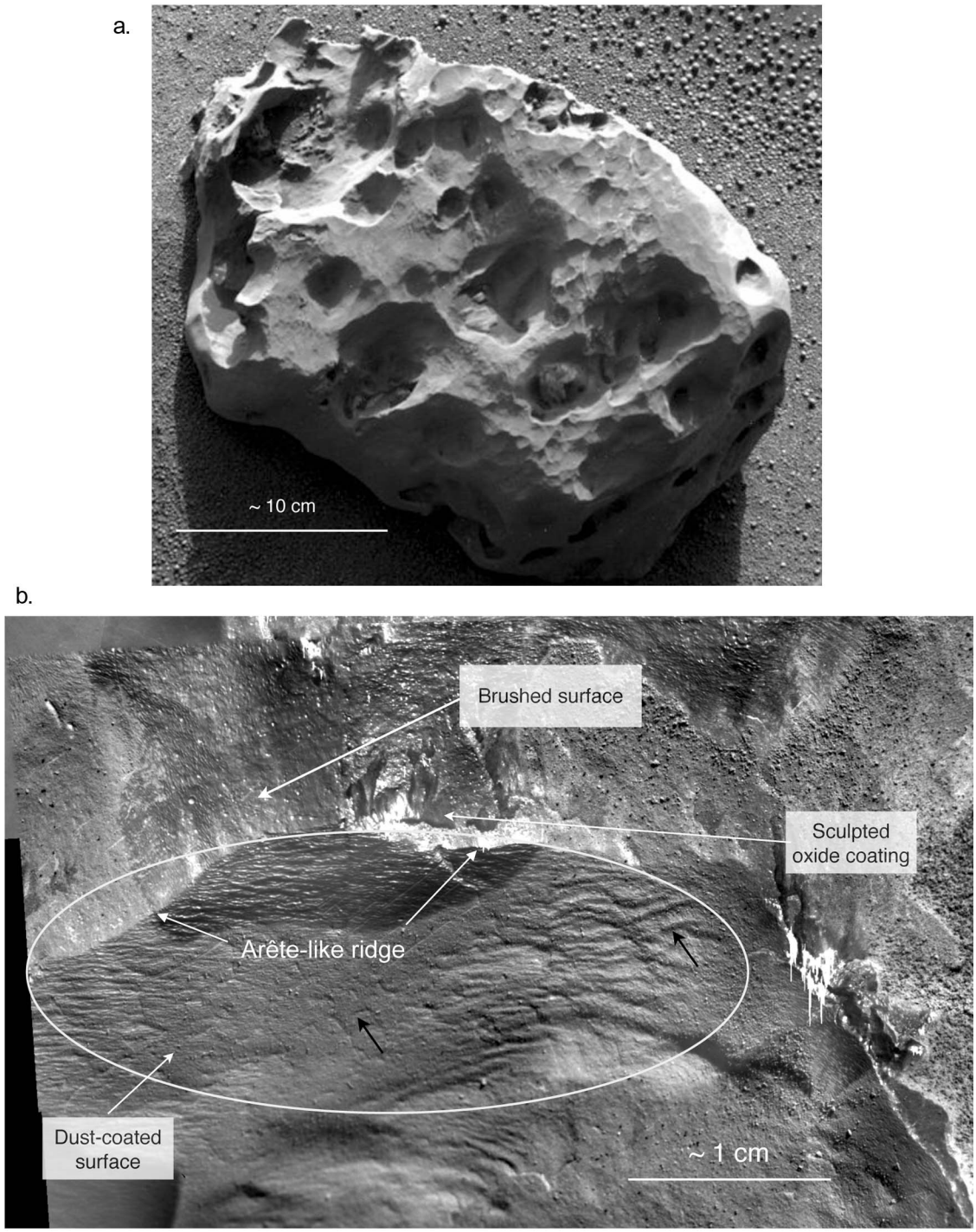

Figure 9. (a) Gray scale Pancam image of the Heat Shield Rock iron-nickel meteorite. (b) Present within and outside the brushed area are sharp-edged, arête-like sculptings of original ablation features together with indications of the Widmanstätten pattern common to cut, polished, and acid-etched iron-nickel meteorites with an appropriate nickel composition (black arrows in Figure 9b). Imperfect kamacite plate alignments result in subparallel expression. All these features suggest postfall mechanical abrasion to greater or lesser amounts. Image credits: NASA/JPL/Pancam/MI.

ablation during entry, we conclude that at least some of the shallow surface hollows are not unmodified regmaglypts. Their occurrence may, however, be controlled in part by the location of regmaglypts, which may offer a preferred path of mass removal to erosive forces and become enlarged with time. An example of troilite nodule size and distribution in a IAB complex meteorite is presented as Figure 11. The nodule indicated by the black arrow marks the edge of the meteorite when recovered, and shows a local hollow that

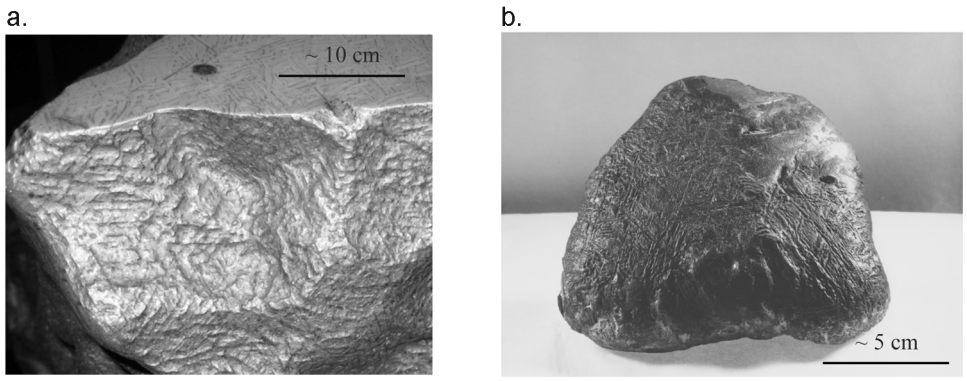

Figure 10. Both the (a) Drum Mountains and (b) Fort Stockton medium octahedrite irons also show definite signs of differential mechanical weathering. Note how Widmanstätten lamellae of sliced and etched uppermost surface of Drum Mountains interfaces with pattern on weathered surface.

may have formed either from atmospheric ablation or differential weathering.

[40] Other forms of anomalous pitting can be found on Shelter Island. Figure 5a shows several hollows that appear to contain smaller-diameter cavities at their bases (black arrows), resulting in a funnel-shaped cross section for the hollow. This type of shape can occur during atmospheric ablation when the ablating hollow (regmaglypt) encounters a less resistant troilite inclusion, which is then removed through the small-diameter orifice at the bottom of the regmaglypt. The weathered feature at the Figure 5c red arrow also suggests the possibility for postfall creation of some of these funnel-shaped hollows. A possible analog for such a process may be present on Earth in places where sand saltation can shape increasingly smaller-diameter borings through a kind of venturi-like acceleration of the erosive sand particles (e.g., Garnet Hill, Mohave Desert, California; Figure 12). Where conditions are favorable, eolian scouring has also been capable of enlarging volumes preferentially, once initiated by originally minor irregularities in an otherwise coarsely homogeneous material.

4.4. General Discussion

[41] The delicate remnant metal structures seen on Shelter Island and Mackinac Island present striking evidence for cavernous weathering processes. The hollowing near their bases is more pronounced than in their upper portions, and has produced a somewhat undercut profile (see Figures 5 and 6). This presumably reflects greater exposure to mass-removing processes in the few centimeters close to the

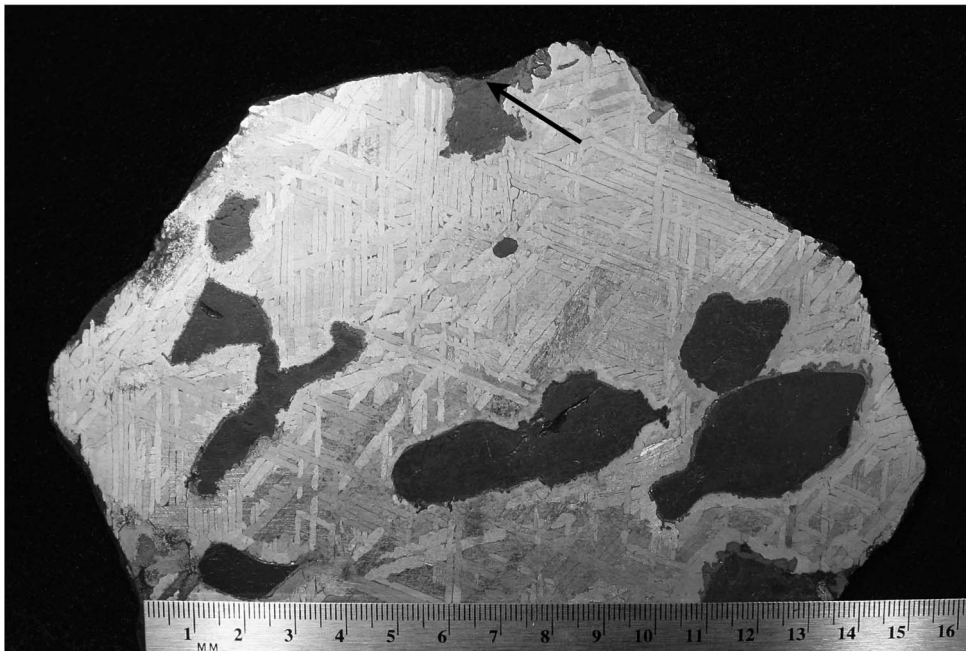

Figure 11. An etched slice of the Toluca IAB complex meteorite showing common size and distribution of troilite (FeS) nodules in this class of iron meteorite. These nodules may offer zones of weakness to weathering forces and account in part for the final morphology of an altered meteorite.

Figure 12. Ventifacted granodiorite, Garnet Hill, Mohave Desert, California. Presented as a potential analog for discussion of funnel-shaped cavity formation; modified rock volume is homogeneous, massive, and unfractured. Wind-blown sand has created smooth-sculpted patterns with smaller-diameter cavities penetrating more deeply into rock, producing funnel-shaped cross sections reminiscent of those found in Shelter Island (see Figure 5a and text for discussion). Coin for scale is 21.75 mm in diameter.

ground than higher above it. It is not obvious whether the process or processes that created these features were aqueous, eolian, or a combination of both. While examples of cavernously weathered iron meteorites can be found on Earth (e.g., the Willamette iron meteorite) [*Pugh and Allen*, 1986], the morphologies are not entirely analogous to what has been found on Mars. In the case of Willamette, large cavities are thought to have formed primarily from sulfuric acid generated from troilite-water interactions, though some atmospheric ablation may have contributed [e.g., *Pugh and Allen*, 1986]. Reaction kinetics, water availability, and exposure time differences between planetary environments undoubtedly play significant roles in determining which processes predominate. Resolving these questions will require further study. Using Willamette as our best available analog, however, our current thinking favors an aqueous explanation for the cavernous weathering found in Shelter Island and Mackinac Island. Notwithstanding the cavernously weathered interiors, the presence of what are likely to be remnant regmaglypts (thumbprint-shaped indentations in Figure 4a) indicates that the Meridiani iron suite probably has undergone only minimal exterior surface modification, and overall shapes may not differ significantly from their original outlines.

[42] The dichotomy in Block Island's surface roughness suggests the possibility of prolonged partial burial at some point during the postfall history of the rock (i.e., the smoother portion appears to have been exposed to more erosion). More recent burial and exposure is evident by the presence of blueberries in the hollows to only ~14 cm above the ground surface (but no higher) in Block Island. This observation suggests that at some time one or more ripples migrated over the meteorite up to this height and left the blueberries behind. The fact that blueberries are not found higher than this elevation provides the maximum crest height for the ripples at the time of migration. These ripples are thought to be currently inactive [*Golombek et al.*, 2010; *Jerolmack et al.*, 2006]. The grain size currently expected to be most easily saltated on Mars is 100–150 μm [e.g., *Greeley et al.*, 1982]. The hoodoo pedestal beneath Block Island suggests that saltating sand removed the weak sulfate bedrock from beneath the meteorite as it rested on its surface. It should be emphasized that calculating residence times for meteorites found on Mars is poorly constrained.

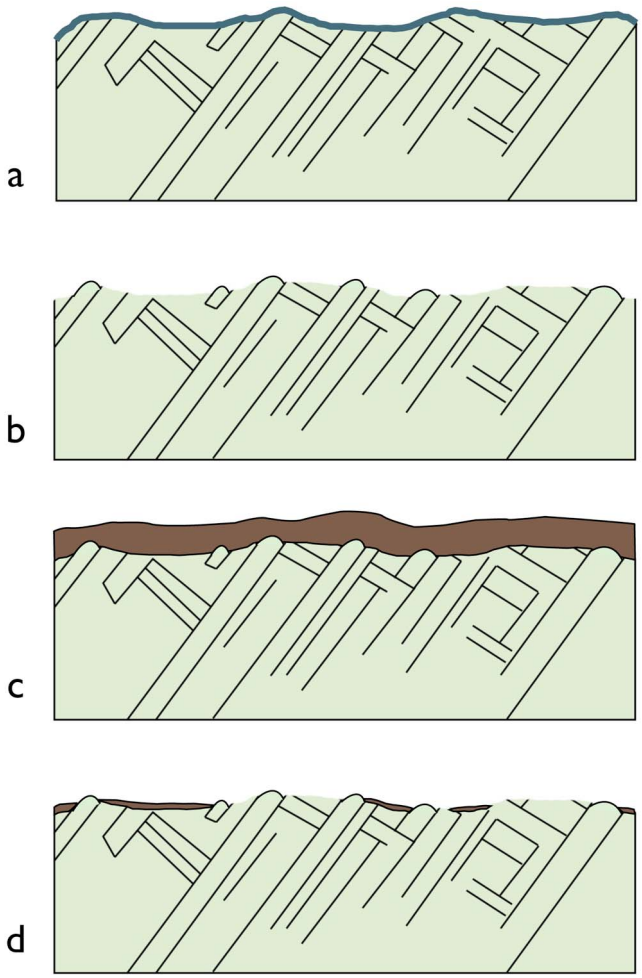

Figure 13. Schematic illustrating possible alteration sequence for surface features observed at New Shoreham in Block Island and Shelter Island based on crosscutting relationships observed in MI mosaics. (a) A regmaglypted meteorite arrives on Mars with a thin fusion crust (blue layer). (b) Subsequent exposure to eolian scouring produces differentially eroded Widmanstätten features and removes the fusion crust entirely; (c) local hollow locations are influenced by original regmaglypted topography. Subsequent exposure to water (possibly ice during burial or high Martian obliquity phase) results in aqueous alteration with oxidized coating (brown layer; thickness is unknown and estimated here for illustration purposes). (d) Additional scouring reduces coating to discontinuous patches with lobate margins and reexposes topographic highs created by Widmanstätten pattern during earlier abrasive epoch.

Since the ripples have been inactive for the past ~100 ka [*Golombek et al.*, 2010], the meteorites must have landed prior to 100 ka. However, there is little to argue against their landing substantially longer ago than that.

[43] Based on crosscutting relationships between the dark coating and differentially eroded taenite lamellae discussed in sections 4.2 and 4.3, respectively, a sequence of surface modification events at New Shoreham on Block Island is suggested in Figure 13. In this scenario, the meteorite arrives on Mars with a thin fusion crust and regmaglypted surface (blue layer in Figure 13a). Subsequent exposure to eolian scouring produces differentially eroded Widmanstätten features and removes the fusion crust entirely (Figure 13b), with regmaglypts influencing the resulting local topography. The meteorite is subsequently exposed to water to produce an oxidized coating of unknown original thickness (Figure 13c). We offer subsurface ice interaction (possibly during ripple migration) as a plausible cause for the production of this dark coating as a weathering product, pursuant to the ice discussion presented in section 2.1 and the findings of *Yen et al.* [2005b]. The process may be enhanced during periods of high obliquity when water ice may also be stable at the surface. Additional scouring reduces the coating to discontinuous patches with lobate margins, and reexposes topographic highs created by the Widmanstätten pattern during the earlier abrasive epoch (Figure 13d).

5. Conclusions

[44] While many questions remain to be answered, the following findings have been made regarding the Block Island, Shelter Island, and Mackinac Island meteorites:

[45] 1. Based on crosscutting relationships with wind-sculpted features and elevated Mg and Zn abundances relative to those of its substrate, the dark (purple hued in false color Pancam images) coating observed on Block Island is not a fusion crust. All indications suggest the coating to be a secondary weathering product. Similar coatings on Shelter Island and Heat Shield Rock are likely to have a similar origin.

[46] 2. At least two episodes of mechanical abrasion have taken place on Block Island. The first of these resulted in the differential erosion of the kamacite-taenite lamellae. The second occurred after deposition of the dark coating.

[47] 3. The presence of hematite blueberries within hollows on each of the three meteorites confirms that ripples have migrated over the meteorites in the past. The height of their location marks the maximum height of the ripples.

[48] 4. Based on the morphology of delicate metal protrusions lining the rim of the cavernous pit on Block Island, which may mark the location of a former inclusive mass, at least one episode of acidic liquid water exposure is plausible for this rock.

[49] 5. The differences in weathering state among the three irons along with different weathering faces (north versus northeast versus northwest) may represent different residence times, burial depths, or environments.

[50] 6. The smooth, rounded shape of most of the meteorite surfaces and similarity of "thumbprint" sculpting to regmaglypts caused by atmospheric ablation suggests the overall size of the meteorites is similar to when they landed on Mars. Erosion since they landed, aside from cavernous weathering, is limited to etching of the surface to expose the Widmanstätten pattern and to elongate and expand hollows by eolian activity.

[51] Continued study of these, Oileán Ruaidh, Ireland, and future meteorites may provide further insights into the details of these processes. The viability of using weathered meteorites as markers for water exposure was outlined as a testable hypothesis for the MERs in particular [*Ashley and Wright*, 2004], but the approach has applications to future Mars missions (and may have relevance to other situations in the solar system generally). As demonstrated by the discovery of meteorites at both MER sites, meteorites are likely to be present in significant numbers across the planet. It is probable that current and future roving spacecraft will continue to encounter meteoritic specimens, and opportunities for further study can be anticipated. Indeed, a case has been made for consideration of such materials in a Mars sample return program, as laboratory analysis of alteration effects will provide the most control for an assessment of subtle aqueous processes (J. W. Ashley et al., The scientific rationale for studying meteorites found on other worlds, available at http://www8.nationalacademies.org/ssbsurvey/DetailFileDisplay.aspx?id=162&parm_type=PSDS, 2009). We recommend consideration of the meteorite problem during mission operations for MSL, as well as when selecting instruments for future rover missions.

[52] **Acknowledgments.** We would like to express our sincerest thanks to our two anonymous reviewers. Jonathan Hill and Eliana McCartney were supportive in the acquisition of data products. Marc Fries was helpful in preliminary discussions. Ella Mae Lee and Bonnie Redding from the USGS team are thanked for assembling the MI mosaics for this paper. Laurence Garvie of Arizona State University's Center for Meteorite Studies is acknowledged for access to meteorite collections and discussions. For the MIPL geometric model of Block Island, we thank Nick Ruoff for tiepointing and localization, Oleg Pariser for meshing, Kris Capraro for masking off bad areas, Zareh Gorjian and Mike Stetson for cleaning up the model and determining the volume, and Bob Deen for overseeing the effort. Funding was provided in part through NASA Graduate Student Researchers Program grant NNX06-AD83H.

References

Ashley, J. W., and M. A. Velbel (1997), Comparison of petrographic, gravimetric, and X-ray diffraction indices of weathering in weathering category C ordinary chondrites from Antarctica, *Meteorit. Planet. Sci.*, *32*, suppl., A9.

Ashley, J. W., and M. A. Velbel (2007), Passivation of metal oxidation by iron oxide production in ordinary chondrites weathered in a Mars analog environment, *Meteorit. Planet. Sci.*, *42*, suppl., 5192.

Ashley, J. W., and S. P. Wright (2004), Iron oxidation products in Martian ordinary chondrite finds as possible indicators of water exposure at Mars Exploration Rover landing sites, *Lunar Planet. Sci.*, *XXXV*, Abstract 1750.

Ashley, J. W., S. W. Ruff, P. R. Christensen, and L. A. Leshin (2008), Effects of dust on thermal infrared reflectivity of iron meteorite candidates found by the Mars Exploration Rovers, *Meteorit. Planet. Sci.*, *43*, suppl., A20.

Ashley, J. W., T. McCoy, and C. Schroder (2009a), Evidence for physical weathering of iron meteorite Meridiani Planum (Heat Shield Rock) on Mars, *Eos Trans. AGU*, *90*(52), Fall Meet. Suppl., Abstract P13A–1248.

Ashley, J. W., S. W. Ruff, A. Trubea Knudson, and P. R. Christensen (2009b), Mini-TES measurements of Santa-Catarina-type, stony-iron meteorite candidates by the Opportunity rover, *Lunar Planet. Sci.*, *XLI*, Abstract 2468.

Baldridge, A. M., and W. M. Calvin (2004), Hydration state of the Martian coarse-grained hematite exposures: Implications for their origin and evolution, *J. Geophys. Res.*, *109*, E04S90, doi:10.1029/2003JE002066.

Bell, J. F., et al. (2003), Mars Exploration Rover Athena Panoramic Camera (Pancam) investigation, *J. Geophys. Res.*, *108*(E12), 8063, doi:10.1029/2003JE002070.

Bibring, J. P., et al. (2005), Mars surface diversity as revealed by the OMEGA/Mars Express observations, *Science*, *307*, 1576–1581, doi:10.1126/science.1108806.

Bibring, J. P., et al. (2006), Global mineralogical and aqueous mars history derived from OMEGA/Mars express data, *Science*, *312*, 400–404, doi:10.1126/science.1122659.

Bibring, J. P., et al. (2007), Coupled ferric oxides and sulfates on the Martian surface, *Science*, *317*, 1206–1210, doi:10.1126/science.1144174.

Birch, W. D., and L. E. Samuels (2003), The Ballarat meteorite, a fossil IAB iron from Victoria, Australia, *Proc. R. Soc. Vic.*, *115*(1–2), 67–75.

Bland, P. A., and T. B. Smith (2000), Meteorite accumulations on Mars, *Icarus*, *144*, 21–26, doi:10.1006/icar.1999.6253.

Bland, P. A., F. J. Berry, and C. T. Pillinger (1998a), Rapid weathering in Holbrook: An iron-57 Mossbauer spectroscopy study, *Meteorit. Planet. Sci.*, *33*, 127–129, doi:10.1111/j.1945-5100.1998.tb01614.x.

Bland, P. A., A. S. Sexton, A. J. T. Jull, A. W. R. Bevan, F. J. Berry, D. M. Thornley, T. R. Astin, D. T. Britt, and C. T. Pillinger (1998b), Climate and rock weathering: A study of terrestrial age dated ordinary chondritic meteorites from hot desert regions, *Geochim. Cosmochim. Acta*, *62*, 3169–3184, doi:10.1016/S0016-7037(98)00199-9.

Bland, P. A., M. E. Zolensky, G. K. Benedix, and M. A. Sephton (2006), Weathering of chondritic meteorites, in *Meteorites and the Early Solar System II*, edited by D. S. Lauretta and H. Y. McSween Jr., pp. 853–867, Univ. of Ariz. Press, Tucson.

Buchwald, V. F. (1973), The pallasite Imilac, Chille, *Meteoritics*, *8*, 333–334.

Buchwald, V. F. (1975), *Handbook of Iron Meteorites*, 1418 pp., Univ. of Calif. Press, Berkeley.

Buchwald, V. F. (1977), The mineralogy of iron meteorites, *Philos. Trans. R. Soc. A*, *286*(1336), 453–491, doi:10.1098/rsta.1977.0127.

Buchwald, V. F., and R. S. Clarke (1988), Akaganeite, not lawrencite, corrodes Antarctic iron meteorites, *Meteorit. Planet. Sci.*, *23*, 261.

Buchwald, V. F., and R. S. Clarke (1989), Corrosion of Fe-Ni alloys by Cl-containing akaganéite (β-FeOOH): The Antarctic meteorite case, *Am. Mineral.*, *74*, 656–667.

Burns, R. G., and S. L. Martinez (1991), Mössbauer spectra of olivine-rich achondrites: Evidence for preterrestrial REDOX reactions, *Proc. Lunar Planet. Sci.*, *21st*, 331–340.

Campbell, I. B., and G. G. C. Claridge (1987), *Antarctica: Soils, Weathering Processes and Environment*, 368 pp., Elsevier Sci., Amsterdam.

Carr, M. H. (1996), *Water on Mars*, Oxford Univ. Press, New York.

Carr, M. H., and J. W. Head III (2003), Basal melting of snow on early Mars: A possible origin of some valley networks, *Geophys. Res. Lett.*, *30*(24), 2245, doi:10.1029/2003GL018575.

Chappelow, J. E., and M. Golombek (2010a), Can Mars' current atmosphere land Block Island sized meteorites?, *Lunar Planet. Sci.*, *XLI*, Abstract 2351.

Chappelow, J. E., and M. Golombek (2010b), Event and conditions that produced the iron meteorite Block Island on Mars, *J. Geophys. Res.*, *115*, E00F07, doi:10.1029/2010JE003666.

Chappelow, J. E., and V. L. Sharpton (2006a), Atmospheric variations and meteorite production on Mars, *Icarus*, *184*, 424–435, doi:10.1016/j.icarus.2006.05.013.

Chappelow, J. E., and V. L. Sharpton (2006b), The event that produced heat shield rock and its implications for the Martian atmosphere, *Geophys. Res. Lett.*, *33*, L19201, doi:10.1029/2006GL027556.

Christensen, P. R. (2003), Formation of recent Martian gullies through melting of extensive water-rich snow deposits, *Nature*, *422*, 45–48, doi:10.1038/nature01436.

Christensen, P. R., and S. W. Ruff (2004), Formation of the hematite-bearing unit in Meridiani Planum: Evidence for deposition in standing water, *J. Geophys. Res.*, *109*, E08003, doi:10.1029/2003JE002233.

Christensen, P. R., et al. (2003), Miniature Thermal Emission Spectrometer for the Mars Exploration Rovers, *J. Geophys. Res.*, *108*(E12), 8064, doi:10.1029/2003JE002117.

Coey, J. M. D., et al. (2002), Ferromanetism of a graphite nodule from the Canyon Diablo meteorite, *Nature*, *420*, 156–159, doi:10.1038/nature01100.

Connolly, H. C. J., et al. (2006), Meteoritical Bulletin #90, *Meteorit. Planet. Sci.*, *41*, 1383–1418, doi:10.1111/j.1945-5100.2006.tb00529.x.

Desch, S. (2006), Meteoritics: How to make a chondrule, *Nature*, *441*, 416–417, doi:10.1038/441416a.

Dodd, R. T. (1981), *Meteorites: A Petrologic-Chemical Synthesis*, Cambridge Univ. Press, New York.

El Goresy, A., and H. Fechtig (1967), Fusion crust of iron meteorites and mesosiderites and production of cosmic spherules, *Smithson. Contrib. Astrophys.*, *11*, 391.

Farrand, W. H., et al. (2007), Visible and near-infrared multispectral analysis of rocks at Meridiani Planum, Mars, by the Mars Exploration Rover Opportunity, *J. Geophys. Res.*, *112*, E06S02, doi:10.1029/2006JE002773.

Feldman, W. C., et al. (2004), Global distribution of near-surface hydrogen on Mars, *J. Geophys. Res.*, *109*, E09006, doi:10.1029/2003JE002160.

Fleischer, I., W. H. Farrand, C. Schröder, B. L. Jolliff, J. W. Ashley, and G. Klingelhöfer (2009), Cobbles at Meridiani Planum, paper presented at European Planetary Science Congress, Eur. Planet. Network, Potsdam, Germany.

Fleischer, I., C. Schröder, G. Klingelhöfer, J. Zipfel, R. V. Morris, J. W. Ashley, and R. Gellert (2010a), New insights into the mineralogy and weathering of the Meridiani Planum meteorite, Mars: Identification of kamacite, taenite, schreibersite, and iron oxides, *Meteorit. Planet. Sci.*, *46*, 21–34.

Fleischer, I., et al. (2010b), Mineralogy and chemistry of cobbles at Meridiani Planum, Mars, investigated by the Mars Exploration Rover Opportunity, *J. Geophys. Res.*, *115*, E00F05, doi:10.1029/2010JE003621.

Fleischer, I., G. Klingelhöfer, C. Schröder, D. W. Mittlefehdt, R. V. Morris, M. Golombek, and J. W. Ashley (2010c), In situ investigation of iron meteorites at Meridiani Planum, Mars, *Lunar Planet. Sci.*, *XLI*, Abstract 1791.

Flynn, G. J., and D. S. McKay (1990), An assessment of the meteoritic contribution to the Martian soil, *J. Geophys. Res.*, *95*, 14,497–14,509, doi:10.1029/JB095iB09p14497.

Golombek, M. P., et al. (2006), Erosion rates at the Mars Exploration Rover landing sites and long-term climate change on Mars, *J. Geophys. Res.*, *111*, E12S10, doi:10.1029/2006JE002754.

Golombek, M., K. Robinson, A. S. McEwen, N. T. Bridges, A. Ivanov, L. L. Tornabene, and R. Sullivan (2010), Constraints on ripple migration at Meridiani Planum from observations of fresh craters by Opportunity and HiRISE, *Lunar Planet. Sci.*, *XLI*, Abstract 2373.

Gooding, J. L. (1978), Chemical weathering on Mars thermodynamic stabilities of primary minerals (and their alteration products) from mafic igneous rocks, *Icarus*, *33*, 483–513.

Gooding, J. L. (1986a), Clay-mineraloid weathering products in Antarctic meteorites, *Geochim. Cosmochim. Acta*, *50*, 2215–2223, doi:10.1016/0016-7037(86)90076-1.

Gooding, J. L. (1986b), Weathering of stony meteorites in Antarctica, paper presented at International Workshop on Antarctic Meteorites, Lunar and Planet. Inst., Houston, Tex.

Gooding, J. L. (1989), Significance of terrestrial weathering effects in Antarctic meteorites, *Smithson. Contrib. Earth Sci.*, *28*, 93–98.

Gooding, J. L., R. E. Arvidson, and M. Y. Zolotov (1992), Physical and chemical weathering, in *Mars*, edited by H. H. Keiffer et al., pp. 626–651, Univ. of Ariz. Press, Tucson.

Gorevan, S. P., et al. (2003), The Rock Abrasion Tool: Mars Exploration Rover mission, *J. Geophys. Res.*, *108*(E12), 8068, doi:10.1029/2003JE002061.

Greeley, R., R. N. Leach, S. H. Williams, B. R. White, J. B. Pollack, D. H. Krinsley, and J. R. Marshall (1982), Rate of wind abrasion on Mars, *J. Geophys. Res.*, *87*, 10,009–10,024.

Gronstal, A., V. Pearson, A. Kappler, C. Dooris, M. Anand, F. Poitrasson, T. P. Kee, and C. S. Cockell (2009), Laboratory experiments on the weathering of iron meteorites and carbonaceous chondrites by iron-oxidizing bacteria, *Meteorit. Planet. Sci.*, *44*, 233–247, doi:10.1111/j.1945-5100.2009.tb00731.x.

Grotzinger, J. P., et al. (2005), Stratigraphy and sedimentology of a dry to wet eolian depositional system, Burns formation, Meridiani Planum, Mars, *Earth Planet. Sci. Lett.*, *240*, 11–72, doi:10.1016/j.epsl.2005.09.039.

Grotzinger, J., et al. (2006), Sedimentary textures formed by aqueous processes, Erebus crater, Meridiani Planum, Mars, *Geology*, *34*(12), 1085–1088, doi:10.1130/G22985A.1.

Harvey, R. (2003), The origin and significance of Antarctic meteorites, *Chem. Erde*, *63*(2), 93–147, doi:10.1078/0009-2819-00031.

Herkenhoff, K. E., et al. (2003), The Athena Microscopic Imager investigation, *J. Geophys. Res.*, *108*(E12), 8065, doi:10.1029/2003JE002076.

Horgan, B. H., J. F. Bell, E. Z. N. Dobrea, E. A. Cloutis, D. T. Bailey, M. A. Craig, L. H. Roach, and J. F. Mustard (2009), Distribution of hydrated minerals in the north polar region of Mars, *J. Geophys. Res.*, *114*, E01005, doi:10.1029/2008JE003187.

Hurowitz, J. A., W. W. Fischer, N. J. Tosca, and R. E. Milliken (2010), Origin of acidic surface waters and the evolution of atmospheric chemistry on early Mars, *Nat. Geosci.*, *3*, 323–326, doi:10.1038/ngeo831.

Huss, G. R., A. P. Meshik, J. B. Smith, and C. M. Hohenberg (2003), Presolar diamond, silicon carbide, and graphite in carbonaceous chon-

drites: Implications for thermal processing in the solar nebula, *Geochim. Cosmochim. Acta*, *67*, 4823–4848, doi:10.1016/j.gca.2003.07.019.

Jerolmack, D. J., D. Mohrig, J. P. Grotzinger, D. A. Fike, and W. A. Watters (2006), Spatial grain size sorting in eolian ripples and estimation of wind conditions on planetary surfaces: Application to Meridiani Planum, Mars, *J. Geophys. Res.*, *111*, E12S02, doi:10.1029/2005JE002544.

Johnson, C. A., W. M. Calvin, W. H. Farrand, K. E. Herkenhoff, R. V. Morris, J. W. Ashley, E. M. Lee, J. F. Bell III, and C. M. Weitz (2009), Pancam multispectral observations of the Block Island meteorite, Meridiani Planum, Mars, *Eos Trans. AGU*, *90*(52), Fall Meet. Suppl., Abstract P13A–1247.

Johnson, J. R., K. E. Herkenhoff, J. F. Bell III, W. H. Farrand, J. W. Ashley, C. Weitz, and S. W. Squyres (2010), Pancam visible/near-infrared spectra of large Fe-Ni meteorites at Meridiani Planum, Mars, *Lunar Planet. Sci.*, *XLI*, Abstract 1974.

Kleine, T., M. Touboul, B. Bourdon, F. Nimmo, K. Mezger, H. Palme, S. B. Jacobsen, Q. Z. Yin, and A. N. Halliday (2009), Hf-W chronology of the accretion and early evolution of asteroids and terrestrial planets, *Geochim. Cosmochim. Acta*, *73*, 5150–5188, doi:10.1016/j.gca.2008.11.047.

Klingelhöfer, G., et al. (2003), The Athena MIMOS II Mössbauer spectrometer investigation, *J. Geophys. Res.*, *108*(E12), 8067, doi:10.1029/2003JE002138.

Laity, J. E., and N. T. Bridges (2009), Ventifacts on Earth and Mars: Analytical, field, and laboratory studies supporting sand abrasion and windward feature development, *Geomorphology*, *105*(3–4), 202–217, doi:10.1016/j.geomorph.2008.09.014.

Landis, G. A. (2007), Observation of frost at the equator of Mars by the Opportunity rover, *Lunar Planet. Sci.*, *XXXVIII*, Abstract 2423.

Landis, G. A. (2009), Meteoritic steel as a construction resource on Mars, *Acta Astronaut.*, *64*(2–3), 183–187, doi:10.1016/j.actaastro.2008.07.011.

Maki, J. N., et al. (2003), Mars Exploration Rover engineering cameras, *J. Geophys. Res.*, *108*(E12), 8071, doi:10.1029/2003JE002077.

Malin, M., K. S. Edgett, L. V. Posiolova, S. M. McColley, and E. Z. Noe Dobrea (2006), Present-day impact cratering rate and contemporary gully activity on Mars, *Science*, *314*, 1573–1577, doi:10.1126/science.1135156.

McCoy, T. J., I. Casanova, K. Keil, and R. Wieler (1990), Classification of four ordinary chondrites from Spain, *Meteorit. Planet. Sci.*, *25*, 77–79.

McLennan, S. M., et al. (2005), Provenance and diagenesis of the evaporite-bearing Burns formation, Meridiani Planum, Mars, *Earth Planet. Sci. Lett.*, *240*, 95–121, doi:10.1016/j.epsl.2005.09.041.

McSween, H. Y. (1989), Chondritic meteorites and the formation of planets, *Am. Sci.*, *77*(2), 146–153.

Mellon, M. T., and B. M. Jakosky (1995), The distribution and behavior of Martian ground ice during past and present epochs, *J. Geophys. Res.*, *100*, 19,357–19,369.

Mellon, M. T., B. M. Jakosky, and S. E. Postawko (1997), The persistence of equatorial ground ice on Mars, *J. Geophys. Res.*, *102*, 19,357–19,369, doi:10.1029/97JE01346.

Mellon, M. T., W. C. Feldman, and T. H. Prettyman (2004), The presence and stability of ground ice in the southern hemisphere of Mars, *Icarus*, *169*, 324–340, doi:10.1016/j.icarus.2003.10.022.

Mischna, M. A., M. I. Richardson, R. J. Wilson, and D. J. McCleese (2003), On the orbital forcing of Martian water and CO_2 cycles: A general circulation model study with simplified volatile schemes, *J. Geophys. Res.*, *108*(E6), 5062, doi:10.1029/2003JE002051.

Mittlefehdt, D. W. (1980), The composition of mesosiderite olivine clasts and implications for the origin of pallasites, *Earth Planet. Sci. Lett.*, *51*, 29–40, doi:10.1016/0012-821X(80)90254-X.

Muñoz, C., N. Guerra, J. Martinez-Frias, R. Lunar, and J. Cerda (2007), The Atacama Desert: A preferential arid region for the recovery of meteorites - Find location features and strewnfield distribution patterns, *J. Arid Environ.*, *71*(2), 188–200, doi:10.1016/j.jaridenv.2007.03.007.

Mustard, J. F., et al. (2008), Hydrated silicate minerals on Mars observed by the Mars reconnaissance orbiter CRISM instrument, *Nature*, *454*, 305–309, doi:10.1038/nature07097.

Nininger, H. H. (1932), The Springwater meteorite, *Am. Mineral.*, *17*, 396–400.

Norton, O. R. (2002), *The Cambridge Encyclopedia of Meteorites*, 354 pp., Cambridge Univ. Press, London.

Nuding, D. L., and B. A. Cohen (2009), Characterization of rock types at Meridiani Planum, Mars using MER 13-filter Pancam spectra, *Lunar Planet. Sci.*, *XL*, Abstract 2023.

Pugh, R. N., and J. E. Allen (1986), Origin of the Willamette meteorite, *Meteoritics*, *21*, 486–487.

Pun, A., T. J. McCoy, K. Keil, and I. E. Wilson (1990), Classification of five new chondrite finds from Roosevelt County, New Mexico, *Meteorit. Planet. Sci.*, *25*, 233–234.

Rieder, R., R. Gellert, J. Brückner, G. Klingelhöfer, G. Dreibus, A. S. Yen, and S. W. Squyres (2003), The new Athena Alpha Particle X-ray Spectrometer for the Mars Exploration Rovers, *J. Geophys. Res.*, *108*(E12), 8066, doi:10.1029/2003JE002150.

Ruff, S. W., P. R. Christensen, T. D. Glotch, D. L. Blaney, J. E. Moersch, and M. B. Wyatt (2008), The mineralogy of Gusev crater and Meridiani Planum derived from the Miniature Thermal Emission spectrometeres on the Spirit and Opportunity rovers, in *The Martian Surface: Composition, Mineralogy, and Physical Properties*, edited by J. F. Bell III, pp. 315–338, Cambridge Univ. Press, New York.

Schiffman, P., R. Zierenberg, N. Marks, and J. L. Bishop (2006), Acid-fog deposition at Kilauea volcano: A possible mechanism for the formation of siliceous-sulfate rock coatings on Mars, *Geology*, *34*(11), 921–924, doi:10.1130/G22620A.1.

Schröder, C., et al. (2006), A stony meteorite discovered by the Mars Exploration Rover Opportunity on Meridiani Planum, paper presented at 69th Annual Meeting of the Meteoritical Society, Abstract 5285, Zürich, Switzerland.

Schröder, C., et al. (2008), Meteorites on Mars observed with the Mars Exploration Rovers, *J. Geophys. Res.*, *113*, E06S22, doi:10.1029/2007JE002990.

Schröder, C., et al. (2009a), Santorini, another meteorite on Mars and third of a kind, *Lunar Planet. Sci.*, *XL*, Abstract 1665.

Schröder, C., J. W. Ashley, I. Fleischer, R. Gellert, G. Klingelhöfer, P. A. de Souza Jr., and A. S. Team (2009b), Meteorites on Mars: Implications from three probably paired meteorite candidates at Meridiani Planum, *Meteorit. Planet. Sci.*, *44*, suppl., A188.

Schröder, C., et al. (2010), Properties and distribution of paired candidate stony meteorites at Meridiani Planum, Mars, *J. Geophys. Res.*, *115*, E00F09, doi:10.1029/2010JE003616.

Schultz, L. (1986b), Allende in Antarctica: Temperatures in Antarctic meteorites, *Meteoritics*, *21*, 505.

Squyres, S. W., et al. (2010), Recent scientific results from Opportunity's traverse toward Endeavour crater, Meridiani Planum, Mars, *Lunar Planet. Sci.*, *XLI*, Abstract 1757.

Squyres, S. W., et al. (2004), The Opportunity Rover's Athena science investigation at Meridiani Planum, Mars, *Science*, *306*, 1698–1703, doi:10.1126/science.1106171.

Squyres, S. W., et al. (2009), Exploration of Victoria crater by the Mars Rover Opportunity, *Science*, *324*, 1058–1061, doi:10.1126/science.1170355.

Timmes, F. X., and D. D. Clayton (1996), Galactic evolution of silicon isotopes: Application to presolar SiC grains from meteorites, *Astrophys. J.*, *472*, 723–741, doi:10.1086/178102.

Tosca, N. J., S. M. McLennan, B. C. Clark, J. P. Grotzinger, J. A. Hurowitz, A. H. Knoll, C. Schroder, and S. W. Squyres (2005), Geochemical modeling of evaporation processes on Mars: Insight from the sedimentary record at Meridiani Planum, *Earth Planet. Sci. Lett.*, *240*, 122–148, doi:10.1016/j.epsl.2005.09.042.

van Niekerk, D., R. C. Greenwood, I. A. Franchi, E. R. D. Scott, and K. Keil (2007), Seymchan: A main group pallasite - Not an iron meteorite, *Meteorit. Planet. Sci.*, *42*, A154.

Velbel, M. A., and J. L. Gooding (1990), Terrestrial weathering of Antarctic stony meteorites: Developments 1985–1989, paper presented at Workshop on Differences Between Antarctic and non-Antarctic Meteorites, Lunar and Planet. Inst., Houston, Tex.

Velbel, M. A., et al. (1991), Terrestrial weathering of Antarctic stony meteorites: Formation of Mg-carbonates on ordinary chondrites, *Geochim. Cosmochim. Acta*, *55*, 67–76, doi:10.1016/0016-7037(91)90400-Y.

Weisberg, M. K., J. S. Boesenberg, and D. S. Ebel (2002), Gujba and origin of the Bencubbin-like (CB) chondrites, *Lunar Planet. Sci.*, *XXXIII*, Abstract 1551.

Weitz, C. M., et al. (2010), Visible and near-infrared multispectral analysis of geochemically measured rock fragments at the Opportunity landing site in Meridiani Planum, *J. Geophys. Res.*, *115*, E00F10, doi:10.1029/2010JE003660.

Wentworth, S. J., E. K. Gibson, M. A. Velbel, and D. S. McKay (2005), Antarctic dry valleys and indigenous weathering in Mars meteorites: Implications for water and life on Mars, *Icarus*, *174*, 383–395, doi:10.1016/j.icarus.2004.08.026.

Wyatt, M. B., and J. H. Y. McSween (2006), The orbital search for altered materials on Mars, *Elements*, *2*(3), 145–150, doi:10.2113/gselements.2.3.145.

Wyatt, M., J. H. Y. McSween, K. L. Tanaka, and J. W. Head III (2004), Global geologic context for rock types and surface alteration on Mars, *Geology*, *32*(8), 645–648, doi:10.1130/G20527.1.

Yen, A. S., et al. (2005a), An integrated view of the chemistry and mineralogy of Martian soils, *Nature*, *436*, 49–54, doi:10.1038/nature03637.

Yen, A. S., D. W. Ming, R. Gellert, B. C. Clark, R. V. Morris, D. Rodionov, C. Schröder, G. Kingelhöfer, and Athena Science Team (2005b), Subsurface weathering of rocks and soils at Gusev crater, *Lunar Planet. Sci.*, *XXXVI*, Abstract 1571.

Yen, A. S., et al. (2006), Nickel on Mars: Constraints on meteoritic material at the surface, *J. Geophys. Res.*, *111*, E12S11, doi:10.1029/2006JE002797.

Zinner, E., L. R. Nittler, R. Gallino, A. I. Karakas, M. Lugaro, O. Straniero, and J. C. Lattanzio (2006), Silicon and carbon isotopic ratios in AGB stars: SiC grain data, models, and the galactic evolution of the Si isotopes, *Astrophys. J.*, *650*(1), 350–373, doi:10.1086/506957.

Zolotov, M. Y., and E. L. Shock (2005), Formation of jarosite-bearing deposits through aqueous oxidation of pyrite at Meridiani Planum, Mars, *Geophys. Res. Lett.*, *32*, L21203, doi:10.1029/2005GL024253.

J. W. Ashley, and P. R. Christensen, Mars Space Flight Facility, School of Earth and Space Exploration, Arizona State University, Tempe, AZ 85287, USA.

I. Fleischer, Institut für Anorganische und Analytische Chemie, Johannes Gutenberg-Universität, D-55099 Mainz, Germany.

M. P. Golombek and T. J. Parker, Jet Propulsion Laboratory, California Institute of Technology, Pasadena, CA 91011, USA.

K. E. Herkenhoff and J. R. Johnson, Astrogeology Science Center, U.S. Geological Survey, 2255 N. Gemini Dr., Flagstaff, AZ 86001, USA.

T. J. McCoy, Department of Mineral Sciences, National Museum of Natural History, PO Box 37012, Smithsonian Institution, Washington, DC 20013, USA.

C. Schröder, Center for Applied Geoscience, Eberhard Karls University, D-72074 Tübingen, Germany.

S. W. Squyres, Department of Astronomy, Cornell University, Ithaca, NY 14853, USA.